Coupling of membrane and photocalytic technologies for selective formation of high added value chemicals

M. Bellardita[a,*], G. Camera Roda[b], V. Loddo[a], F. Parrino[a], L. Palmisano[a]

[a]"Schiavello-Grillone" Photocatalysis Group, Dipartimento di Energia, Ingegneria dell'informazione, e modelli Matematici (DEIM), University of Palermo, Viale delle Scienze, 90128 Palermo, Italy

[b]Department of Civil, Chemical, Environmental, and Materials Engineering, University of Bologna, via Terracini 28, Bologna (40131), Italy.

*Corresponding author: Marianna Bellardita, E-mail: marianna.bellardita@unipa.it

Abstract

This review presents a survey of some heterogeneous photocatalytic processes for the synthesis of high value added compounds carried out in photocatalytic membrane reactors (PMRs). The two technologies can be easily integrated due to the similar conditions at which they usually operate. Furthermore, significant advantages derive from the coupling and in some cases also synergistic effects can be observed. These features have been highlighted for the photocatalytic syntheses reviewed along with engineering and design aspects investigated for some industrially relevant high value added compounds. Notably, photocatalytic syntheses carried out in PMRs are still rare mainly because interdisciplinary competences and collaborations are often required in this field. However, we hope that a survey of the recently reported examples may inspire researchers for future developments and new opportunities.

Keywords

Heterogeneous photocatalysis; Membrane separation; Photocatalytic membrane reactors; Photocatalytic synthesis.

1. Introduction

Till now, heterogeneous photocatalysis has been mainly applied for environmental remediation because the photogenerated active species are capable to mineralize efficiently almost every organic pollutant. Applications in the field of chemical synthesis remain still rare even if the number of reports concerning new photocatalytic processes for the production of valuable compounds such as drugs, vitamins, fragrances, etc., is rapidly growing. A large variety of reactions has been reported, including oxidations [1-8], reductions [9-15], isomerizations [16], additions [17], cyclizations [18] etc.

As a matter of fact, traditional industrial processes in this field do not often meet the current requirements for sustainability, environmental safety and energy efficiency necessary for a "green" process [19]. For this reason heterogeneous photocatalysis has been proposed as a promising tool for alternative synthetic routes. On the other hand, poor selectivity and high costs related to the separation of the dispersed photocatalyst are the major drawbacks which hinder the industrial application of heterogeneous photocatalysis in this field. Similar issues must be faced for the photocatalytic hydrogen production. Indeed, the low yields of the process due to the fast backward reaction of H_2 to H_2O strongly hinder its practical application.

Coupling photocatalysis with a membrane separation process has been demonstrated to be a viable solution for these problems. Furthermore, photocatalysis and membrane separation can be straightforwardly integrated due to the similar conditions at which they usually operate (relatively low temperature and pressure, and low concentration of the chemicals). However, the research in the field of photocatalytic membrane reactors (PMRs) for synthetic purposes may be still considered at a nascent stage, being PMRs mainly used for environmental remediation. Notably, the study and analysis of PMRs require interdisciplinary competences and collaborations. Also engineering issues should be deeply investigated in order to prove the real viability of PMRs for the synthesis of valuable products.

The number of photocatalytic syntheses performed in PMRs is not yet high, and in the present review we collected all of those that, to the best of our knowledge, have been presented so far. The aim is to give a survey of possible utilizations of PMRs in the chemical synthesis, which can inspire further developments as well as new opportunities.

The first part of the review deals with oxidation reactions while reduction reactions are the subject of the second part. Among the photo-oxidation reactions, the synthesis of phenol from benzene, the partial oxidation of aromatic alcohols to the corresponding aldehydes and the synthesis of vanillin have been reviewed. For this latter reaction, particular attention has been paid to some engineering and design aspects, which have been recently investigated due to the high economical relevance of this flavour compound. CO_2 reduction, H_2 production, nitrite reduction to ammonia and the

synthesis of phenylethanol are the reduction photocatalytic reactions which have been carried out in PMRs. All of these applications are based on a simple common idea. In many cases the product of interest, once photocatalytically generated, is continuously separated from the reacting mixture by means of suitable membranes in order to avoid its overreaction and to endow the process with higher selectivity and efficiency. Indeed, the target compound is generally a reaction intermediate and, as such, its concentration reaches a maximum at the optimum reaction time, before its degradation becomes faster than its generation. Other important benefits of the integration of photocatalysis and membrane separation are (i) the complete retention of the photocatalytic powder in the reacting mixture, thus allowing its continuous utilization and avoiding the post-process separation, and (ii) the possible purification of the product. Positive features of PMRs include the possibility of operating in a continuous or semi-continuous mode, simple process control and modularity.

2. High added value chemicals obtained by oxidation reactions

2.1. Photocatalytic oxidation of benzene to phenol

Phenol is an industrially relevant commodity primarily used in the synthesis of plastics and related materials but also in the production of polycarbonates, epoxides, nylon, detergents, herbicides, and numerous drugs [20,21]. Today phenol is produced on a large scale (about 7 billion kg $year^{-1}$) mainly through the so called "cumene process" which involves the partial oxidation of cumene according to the following reaction:

$$C_6H_5CH(CH_3)_2 + O_2 \rightarrow C_6H_5OH + (CH_3)_2CO \quad (1)$$

Compared to other production alternatives, the cumene process uses relatively mild synthesis conditions, and quite inexpensive raw materials. However, to operate economically, the market demand also for the acetone by-product should be high. This economical requirement, along with the not negligible ecological impact, the presence of an explosive intermediate (cumene hydroperoxide), and the numerous reaction steps necessary, makes green and one-pot alternatives highly desirable [22,23]. In particular the photocatalytic way seems to be quite appealing for its "green" features and for its capability to directly hydroxylate benzene in one step and under mild experimental conditions, by using oxygen as the primary oxidant. However, this reaction has a low selectivity, because phenol is more reactive than benzene and by-products can be formed from further hydroxylation or ring opening [24-29]. Furthermore, the use of a solid photocatalyst (even if cheap, abundant and safe) requires a costly post-process separation. In order to overcome these problems, Molinari et al. [30] investigated the direct benzene conversion to phenol (see Eq. 2) in a hybrid photocatalytic membrane reactor in the presence of TiO_2 as the suspended catalyst.

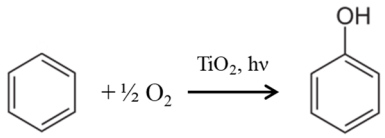

(2)

The experimental set-up is schematically shown in Figure 1.

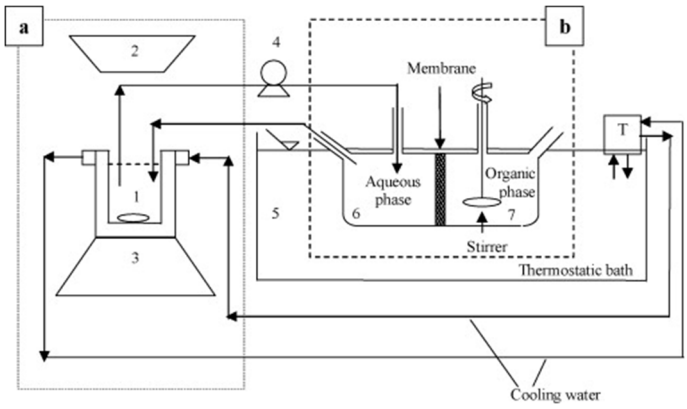

Figure 1. Experimental set-up for oxidation of benzene to phenol: photocatalytic reactor (a) coupled with the membrane contactor (b).
1: batch reactor, 2: UV lamp, 3: magnetic stirrer, 4: peristaltic pump. Reproduced with permission from Ref. [30].

Experimental details can be found in [30]. Briefly, the system consisted of a membrane contactor module coupled with a batch photocatalytic reactor through a recycle loop between them. The aqueous reacting suspension, magnetically stirred and irradiated from the top, flowed through the first compartment of the separation module (compartment 6, Figure 1) where it came into contact with a flat sheet polypropylene membrane. The membrane separated the reacting suspension from a second compartment (7, Figure 1) which contained benzene working as an extracting solvent. Benzene acted both as reactant (permeating from the organic phase to the aqueous phase) and as extraction solvent (phenol, once produced in the reacting mixture, permeated to the organic phase).

The catalyst concentration was a key parameter of the process. Indeed, at a TiO_2 mass concentration of 1 g L^{-1} a high benzene conversion and an efficient light absorption were obtained. However, the effective recovery of phenol by the available membrane with a given area suggested to operate with a lower catalyst concentration (0.1 g L^{-1}) which allowed to reduce fouling phenomena.

The highest phenol production was obtained at alkaline pH values, because phenol interactions with the TiO_2 surface are weakened thanks to the negative charge of both phenolate ions and the nature of the catalyst surface. As a consequence, the further oxidation of phenol to by-products like benzoquinone, hydroquinone and other oxidized molecules resulted to be low and higher selectivity could be achieved.

From these results it is evident that in order to scale up the process, the ratio between the rate of photocatalytic phenol production and that of phenol permeation through the membrane should be carefully chosen also by means of economic evaluations.

The presence of salts and iron(III) dissolved in the aqueous phase was capable to double the phenol flux in the organic phase. Indeed, the enhanced ionic strength of the aqueous phase increased the activity of phenol, thus improving the driving force for permeation [31]. On the other hand, iron(III) enhanced the benzene oxidation rate acting as electron acceptor and facilitating spatial separation of the photogenerated charges [32]. Furthermore the generated iron(II) could initiate photo-Fenton reactions with peroxidic species formed during the photocatalytic process, thus producing additional OH radicals [33].

2.2. Photocatalytic oxidation of primary aromatic alcohol to the corresponding aldehydes

Aromatic aldehydes are valuable compounds used for the preparation of fragrances, food additives, and many organic intermediates [34].

Catalytic partial oxidation of alcohols to the corresponding aldehydes is usually carried out in harmful organic solvents, at high temperatures and pressures and by using stoichiometric amounts of strong inorganic oxidants as chromate and permanganate species. These operating conditions are not only expensive but also produce large amounts of toxic wastes, so that safer and cheaper synthetic routes have been investigated.

In particular, it has been demonstrated that aromatic aldehydes can be photocatalytically produced by partial oxidation of the corresponding alcohols [35-38] under mild conditions, by using water as the solvent and molecular oxygen as the primary oxidant.

Notably, although the reaction was carried out at the best operating conditions, the produced aldehyde could be successively further oxidized. So, a maximum of the aldehyde concentration was reached at an optimal reaction time in a typical photocatalytic experiment (Figure 2).

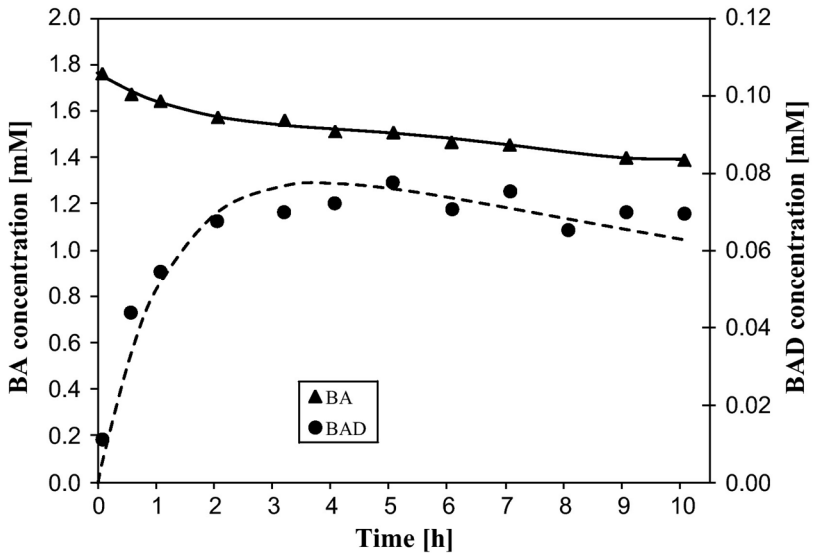

Figure 2. Concentration profiles of benzyl alcohol (BA, triangles) and benzaldehyde (BAD, circles) vs. irradiation time for a typical photocatalytic experiment. Reproduced with permission from Ref. [38].

The higher the ratio of the kinetics of aldehyde degradation to the kinetics of its formation, the lower the yield was. Other problems were related to the intrinsic difficulties of operating in a continuous mode and to the required separation of the photocatalytic powders. Although good selectivity towards aldehydes has been reported, the optimization of the reaction yield and the above mentioned issues have been approached by integrating the reaction with a membrane process [38,39]. Pervaporation was very suitable for this coupling. The aldehyde selectively could permeate through a non-porous membrane from the liquid retentate (reaction side) to the vapour permeate thanks to a solution-diffusion mechanism [40]. Pervaporation presents the advantage that the operating conditions are highly compatible with those of photocatalysis and the valuable aldheydes may be separated with a higher degree of purification.

The experimental set-up is shown in Figure 3.

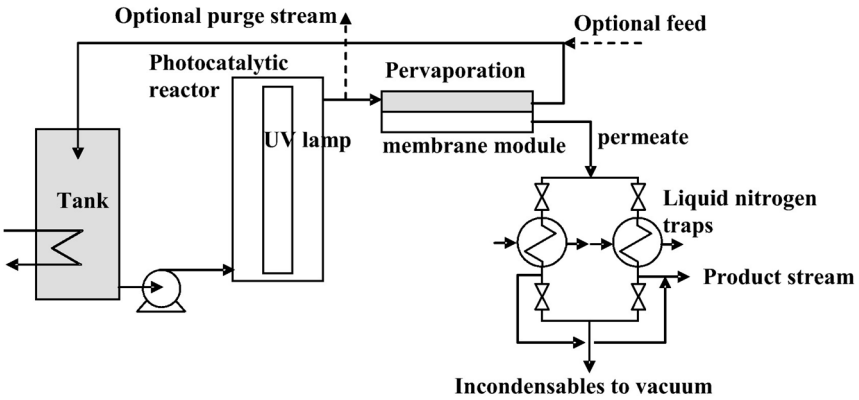

Figure 3. Scheme of the experimental apparatus for alcohol photocatalytic partial oxidation coupled with pervaporation. Reproduced with permission from Ref. [38].

Experimental details can be found in [38]. Briefly, the retentate was recirculated to the annular photoreactor by a peristaltic pump, while the permeate was condensed at low pressure by means of liquid nitrogen traps. Evonik P25 TiO_2 was the photocatalyst suspended in aqueous solution of 4-methoxybenzyl alcohol. 4-Methoxybenzaldehyde has been efficiently separated and concentrated in the permeate, whereas the membrane showed a very good rejection to the alcohol. The suspended photocatalyst was completely separated from the permeate which was always powder-free. Furthermore, the presence of the powder in the reaction side did not affect the membrane performance and both the transmembrane flux and the separation factor were not affected by fouling even after long operating times.

The yield of the sole photocatalytic process reached a plateau and then slowly decreased with time, whereas it monotonically increased after coupling photocatalysis with pervaporation, provided that the membrane area was sufficiently high. Furthermore, aldehyde may compete with alcohol for oxidation so that its recovery in the permeate is beneficial for the rate of the process. Therefore, the conversion of the integrated system was always higher than the conversion obtained for the process without pervaporation.

The selectivity of the sole photocatalytic process continuously decreased with the irradiation time, because of the consecutive reactions. On the contrary, in the integrated system, the rate of the consecutive reaction was depressed by the continuous removal of aldehyde. These outcomes are summarized in Figure 4.

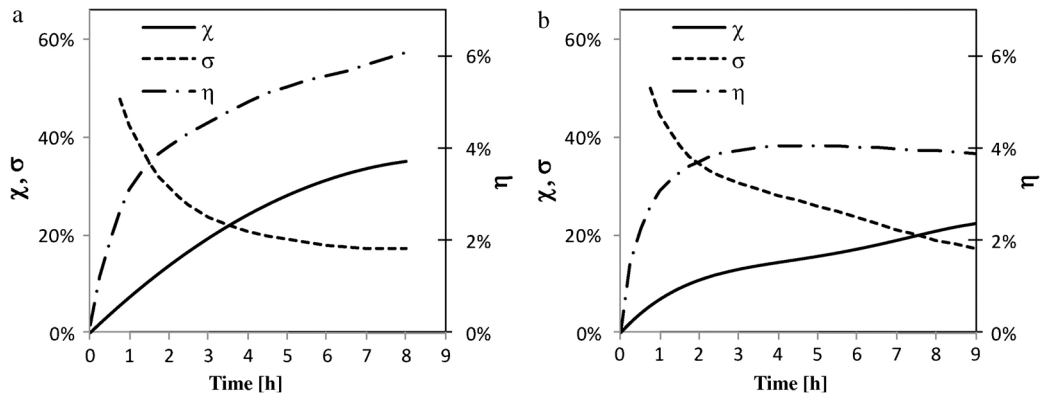

Figure 4. Conversion (χ), selectivity (σ), and yield (η) obtained during the photocatalytic partial oxidation of benzyl alcohol to benzaldehyde with (a) and without (b) the separation step by means of pervaporation. Reproduced with permission from Ref. [38].

The benefits obtained with the integrated process were magnified at high membrane area, because of the higher ratio of the rate of permeation to the one of reaction.

2.3. Photocatalytic oxidation of ferulic acid to vanillin

Vanillin is known as the most important aroma in the world, widely used as flavouring additive in food, cosmetic, pharmaceutical and nutraceutical products [41]. Its annual production, of about 12000 tons [42], mostly derives from chemical syntheses starting from lignosulfonates obtained from the paper industry or from guaiacol of petrochemical derivation. Vanillin extracted from the pods of vanilla planifolia represents only a small fraction (less than 1%) of the global production. Moreover, natural vanillin can not satisfy the increasing demand of the natural product, because of logistic, political and technical problems [43,44]. Therefore, scientific efforts are now directed towards the search of alternative routes for the production of "green" or "natural" vanillin. Indeed, even if the product is totally "natural", the time demanding and laborious curing and extraction process makes the final costs two orders of magnitude higher at least than the one of the synthetic vanillin, and consequently the utilization is restricted to selected products. Actually, the current regulatory guidelines allow to label as "natural", besides the product obtained from the cultivated plants, only the vanillin produced via biotechnological method, regardless the quality of the final product and the sustainability and the eco-friendliness of the process. So, the only "natural" vanillin [45] industrially produced and currently present in the market is Rhovanil natural®. Despite its relatively high cost, deriving from an accurate control of the process, the necessity of selected strains of microorganisms and the complex purification steps, the product has been satisfactorily accepted by the market [46].

Böddeker and coworkers [47-49] demonstrated that polyether-block-amide (PEBA) pervaporation membranes are suitable for permeating fragrances and, in particular, vanillin. Also polyoctyl-methylsiloxane (POMS) membranes have been proposed [50] for the same purposes. The same authors hypothesized vanillin recovery from the reacting broth of the biotechnological synthetic process, both for purification purposes and in order to limit the inhibition effect of vanillin on the biological reaction.

However, fermentation and pervaporation are difficult to integrate due to biofouling on the membrane surface and to the low permeate flux which can be obtained at the relatively low temperatures compatible with the survival of microorganisms. These factors pose severe limitation and hinder a real application of the integrated process.

On the other hand, pervaporation and photocatalysis are perfectly compatible since mild conditions and diluted aqueous solutions represent normal working conditions for both the processes [51].

Augugliaro et al. [52] reported the photocatalytic synthesis of vanillin through oxidation of precursors of natural origin as trans-ferulic acid, isoeugenol, eugenol or vanillyl alcohol. The reaction proceeds in aqueous medium, at room temperature, and by using different TiO_2 samples as the photocatalysts. Selectivity values towards vanillin range from 1.4 to 21 mol%, depending on the substrate and on the type of photocatalyst.

The produced vanillin is separated and recovered with high purity by means of pervaporation coupled with the photocatalytic reaction in a system similar to that shown in Figure 3 and previously described.

The permeation with non-porous PEBAX®2533 membrane took place with high selectivity towards vanillin. The continuous removal of the produced vanillin from the irradiated suspension avoided its subsequent oxidation, thus increasing the process selectivity. Complete retention of the photocatalytic powders with no fouling effects was observed. Part of the permeated vanillin was then recovered as crystals with a high degree of purity ($\geq$ 99.8%) by deposition at temperatures around 0 °C and at the permeate pressure, without the necessity of using complex extraction and re-crystallization procedures.

The vanillin enrichment factor (β_V), which is the ratio of the concentration of the permeating compound upstream the membrane to the one in the condensed permeate, was equal to 4.2. So, the permeate is 4.2 times "enriched" with vanillin with respect to the reacting mixture. Notably, only vanillin, and of course water, permeated at a non-negligible extent. Retention was extraordinarily high for all of the other known and unknown compounds photocatalytically produced and for the reactant ferulic acid. The very low permeation of ferulic acid was mainly due to its low volatility rather than to its dissociation into charged species at the pH of the reacting mixture (pH = ca. 4).

The effect of the temperature has been also evaluated. In pervaporation, relatively high temperature favours the permeability, especially for high boiling compounds, such as vanillin [53]. On the other hand, high temperatures reduce the dissolved oxygen concentration and the adsorption of the substrates thus negatively affecting the photocatalytic reaction rate. Anyhow, negligible effects on the selectivity of the reaction have been observed between 40 and 60 °C. By weighting opportunely the pros and the cons, it was established that about 60 °C represents the most appropriate temperature.

The system used for the production and recovery of vanillin is schematically represented in Figure 5. It is evident that coupling between the reaction and the pervaporation units was ensured by means of recirculation, streams 4 and 5, in a closed loop.

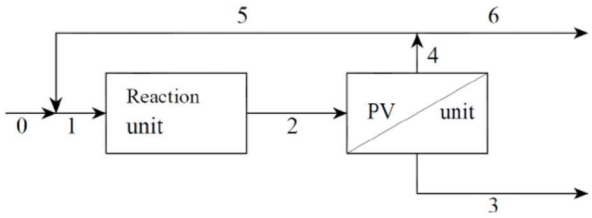

Figure 5. Schematic representation of the coupled photocatalysis-pervaporation system for the synthesis and separation of vanillin.

Configurations in which the two units coexist in a single apparatus have been also proposed. However using separate equipments avoided some possible drawbacks. For example, it has been observed that the direct UVA irradiation of the membrane, in the presence of the photocatalyst, significantly shortened its life time. The use of a single apparatus implies also other inconveniences which will be discussed later. On the other hand, even with the configuration shown in Figure 5 it is possible to obtain a satisfactory integration between the two unit operations. This issue has been systematically investigated [54-56]. The integration is effective if the recirculation flow rate is sufficiently high to ensure that the two units work in a differential way [57].

The vanillin production in the reaction unit and its permeation in the pervaporation unit have been modelled [54].

The photocatalytic production of vanillin is the result of a complex pathway with various parallel and consecutive reactions and different reaction by-products, leading eventually to complete mineralization [52]. A simplified model (Eqs. 3-5) has been proposed in order to reproduce with good reliability the concentration versus time of the compounds of interest, i.e. vanillin (V) and ferulic acid (F). By products derived from oxidation of ferulic acid and of vanillin have been labelled as B and O, respectively. In practice, all of the reactions occur with a first order kinetics.

$$F \rightarrow V \quad (3)$$

$$F \rightarrow B \quad (4)$$

$$V \rightarrow O \quad (5)$$

Mass balances in the reactor and in the pervaporation unit constitute a set of ordinary differential equations which have been numerically solved. Figure 6 shows the amount of vanillin detected in the reaction unit and collected in the permeate during an experiment (points), along with the values predicted by the model (lines). The model satisfactorily fits the experimental data.

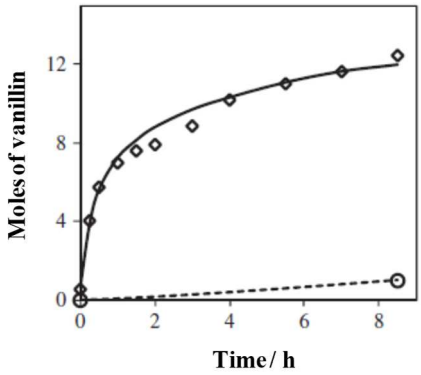

Figure 6. Amount of vanillin present in the reacting solution (◊) and cumulatively collected in the permeate (○) vs. reaction time, along with the respective values predicted by the model (solid line for the reacting solution and dashed line for the permeate).

The integration of the reaction and the separation process allows to increase the yield of the whole process η, which is defined as:

$$\eta = \frac{n_{V,react} + n_{V,perm}}{n_{F,0}} \quad (6)$$

Where $n_{V,react}$ and $n_{V,perm}$ are the moles of vanillin in the reacting suspension and collected in the permeate, respectively, and $n_{F,0}$ are the initial moles of ferulic acid. Generally, in the absence of the recovery of vanillin, its yield reached a maximum and then it decreased with the reaction time [58] due to

its further oxidation. On the other hand, in the integrated system the concentration maximum was lower and more pronounced when the rate of degradation of vanillin was high, i.e. when vanillin was not efficiently removed by pervaporation. Therefore, the yield increased monotonically with the reaction time, when the rate of recovery of vanillin was high with respect to the rate of its formation. The relevant parameter is the ratio of the characteristic rate of permeation to the characteristic average rate of the reaction, which, ultimately affects the performance of the integrated process. This parameteter, δ, can be expressed as:

$$\delta = \frac{(\dot{m}_V/\rho)}{k_1}\frac{A}{V_R} \quad (7)$$

Where $\dot{m}''_V$ (kg h^{-1} m^{-2}) represents the mass flux of the permeate, A (m^2) the area of the membrane, ρ (kg L^{-1}) the density of the condensed permeate, k_1 the apparent kinetic first order constant (h^{-1}) of the vanillin formation (Eq. 1), and V_R (L) the volume of the reactor.

By varying for instance A or V_R, it is possible to operate at different δ values and to evaluate the effects on the yield. In the experiment of Figure 6, it is apparent that the amount of vanillin cumulatively recovered by pervaporation is only a small fraction of the quantity present in the system. By taking into account that the flux and enrichment factor for vanillin are satisfactory, the low amount of vanillin recovered is due to the low value of the ratio of the membrane area to the reactor volume (A/V_R) used in the experiment, which appears in Eq. 7. The variation of the ratio A/V_R, i.e. δ, affects significantly the maximum obtainable yield, η_{max}, as shown in Figure 7.

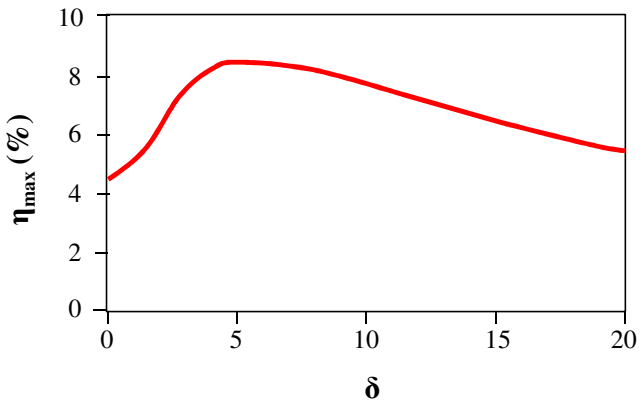

Figure 7. Maximum yield obtained as a function of δ.

The maximum yield obtained for the sole photocatalysis without pervaporation (δ = 0) is 4.46%. The yield increases with δ because vanillin is more efficiently removed from the reaction mixture. However, beyond a certain value of δ an excessive depletion of the reacting suspension takes place. This phenomenon limits the reaction conversion and consequently the yield. These considerations justify the maximum (8.48%) which is obtained at δ_{opt} = 5.7. The maximum value represents a 90% enhancement with respect to the maximum yield that can be obtained with the sole photocatalysis. In other words, the coupling the two technologies implies a substantial "process intensification" [59].

Camera Roda et al. [55] investigated how the yield of the process is influenced by the membrane area (A) and by the enrichment factors (β) of vanillin and ferulic acid. Dimensional analysis applied to the vanillin mass balance in the membrane unit identifies the Péclet number as an important parameter. For a membrane process its definition is:

$$Pe = \frac{\dot{V}_0}{(\frac{A\dot{m}''}{\rho})} = \frac{\dot{V}_0}{\dot{V}_3} \quad (8)$$

where ρ is the density of the condensed permeate, $\dot{m}''$ is the total mass flux of the permeate through the membrane $\dot{V}_0$ and $\dot{V}_3$ are the volumetric flow rates of the streams fed to the system and of the permeate, respectively (see Figure 5). The present definition of the Péclet number is consistent with the one commonly adopted in membrane processes [60,61]. Indeed, Pe represents the ratio of the convective transport to the permeation rate through the membrane. Notably,1/Pe can be interpreted also as a dimensionless membrane/surface area and may vary between 0 and 1. Usual values of 1/Pe are generally in the range between 0 and 0.9.

$$0 \leq 1/Pe \leq 1 \quad (9)$$

1/Pe is 1 when the membrane area is so high to attain a flow rate of the permeate equal to the flow rate of the fresh feed to the system ($\dot{V}_3 = \dot{V}_0$ and $\dot{V}_6 = 0$), whereas 1/Pe equal to 0 represents the case of a photocatalytic reactor without pervaporation ($\dot{V}_3 = 0$ and $\dot{V}_6 = \dot{V}_0$). If the permeate flux is enhanced, a lower membrane area is sufficient to achieve a certain value of 1/Pe. The effects of 1/Pe on the maximum yield were studied by the mathematical model with and without coupling the pervaporation unit and at different enrichment factors of vanillin. The results are shown in Figure 8.

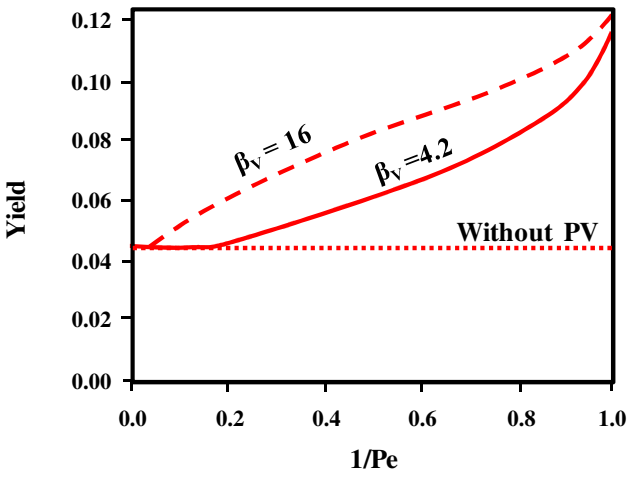

Figure 8. Maximum yield of the process vs the reciprocal of the Péclet number for the coupled system with enrichment factor of vanillin $\beta_V = 4.2$ (solid line) and $\beta_V = 16$ (dashed line) and for the sole photocatalytic system (dotted line).

It can be noticed that: (i) the maximum yield increases with 1/Pe, i.e. with the membrane area; and (ii) below a given value of the membrane area (at ca. 1/Pe = 0.2) no benefit is obtained by the coupling. The yield has been calculated by assuming two different values of the enrichment factor, β_V = 4.2 and β_V = 16. When 1/Pe =1 (large membrane area) the maximum yield passes from 0.1194 for β_V = 4.2 to 0.1235 for β_V = 16 with a small 3.5% increase. However, for intermediate values of 1/Pe, the yield enhancement becomes more important. At the same time, a higher vanillin enrichment factor provides significant savings in membrane area to get a given yield.

A high rejection of ferulic acid, which requires an enrichment factor β_F significantly less than 1 [62], is advantageous as it reduces reactant losses and enhances the conversion. Figure 9 shows the effect of a change of the enrichment factor of the reactant (ferulic acid) from 0.005 to 1 on the maximum yield. The advantages of a high rejection are more important when the membrane area is high (1/Pe ~ 1).

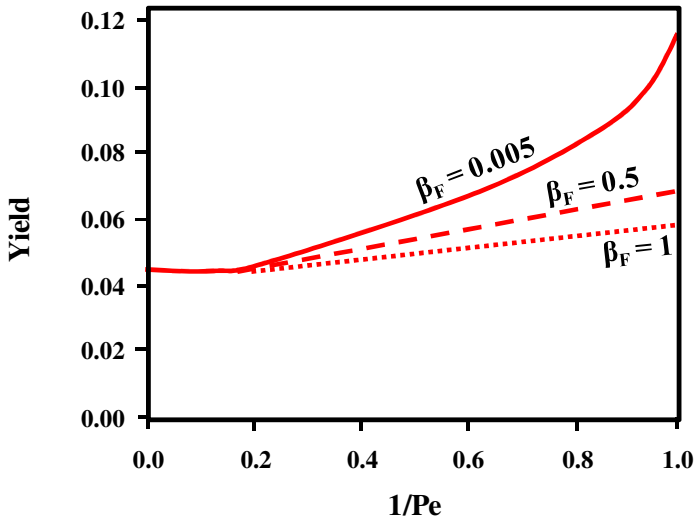

Figure 9. Effect of the enrichment factor of ferulic acid on the dependence of the yield on the reciprocal of the Péclet number.

In summary, process simulation shows that it is important to choose or to develop membranes that selectively permeate the product ($\beta_V >> 1$), while retaining the reactant ($\beta_F << 1$). Furthermore, it is not sufficient that the membrane selectively separate the target compound from the reactant, but it is also advantageous a relatively high vanillin permeate flux since it allows to operate at high values of 1/Pe, even with a limited membrane area.

The study of the vanillin pervaporation with PEBAX membranes shows that β_V increases with the membrane thickness. Indeed, the vanillin flux through the membrane slightly depends on the membrane thickness, while the water flux is inversely proportional to the membrane thickness.

An improvement of β_V can be obtained by raising the temperature, with the additional positive effect of increasing the vanillin flux.

Vanillin permeation is affected by pH, being relatively high when vanillin is not dissociated (pH < 6.5), but decreasing when most of vanillin is dissociated. On the other hand, pH has a minor influence on the rejection of ferulic acid, which remains high also at low pH values, when the substrate in solution is undissociated. The real reason for the very high rejection of the substrate (ferulic acid) and of most of the by-products is the low volatility of these compounds. Indeed, preliminary experiments in a dialysis process, i.e. with an aqueous solution on both sides of the membrane (so that permeation takes place without evaporation of the permeate), showed that the flux of vanillin becomes ten times greater than in pervaporation and the ferulic acid flux becomes comparable with that of vanillin. These latter results show that: (i) all the aromatic compounds involved in the synthesis of vanillin can easily diffuse through the membrane; (ii) the low volatility of the higher boiling compounds gives rise to their high retention in pervaporation; and (iii) in pervaporation, the permeation of vanillin is somehow limited by its relatively low volatility.

By summarizing, process simulation shows that the main requisites for an efficient integrated process are: (i) high β_V, whose main effect is to enhance the yield and/or to reduce the required membrane area; (ii) high rejection of the reactant, whose main effect is to enhance the conversion and to reduce the required volume of the reactor; and (iii) a relatively high flux of vanillin, whose main effect is to reduce the required membrane area for a given yield or to increase the yield for a given membrane area.

The integration of the two processes can take place inside a single apparatus or using separate units. Even if using a single apparatus results in a direct coupling, separate units offer higher degrees of freedom for the design and larger possibilities for the optimization of the system. For instance, in the specific case of photocatalytic membrane reactors, separated units allow to avoid the direct irradiation of the membrane which may be damaged in long term operations. However, the integration of the two unit must be maintained and optimized in order to maximize the efficiency of the whole process. Recently, Camera Roda et al. [56] reported the influence of two parameters on the "degree" of integration between the reaction and the pervaporation units: (i) the recycle ratio, R, defined as the ratio between the flow rate recirculating from the separation unit to the reaction unit (stream 5 in Figure 5) and the flow rate entering the reaction-separation units (stream 1 in Figure 5); and (ii) the number N of reaction-separation units in which the whole process can be fractionated. Furthermore, with separated apparatuses the reactor volume and the membrane area can be changed at will without any constrain and the hydrodynamic conditions optimized for each individual process.

R may vary from 0 (no recycle) to 1 (total backmixing).

The performance obtained for R→1 approaches that of a continuously stirred tank reactor (CSTR) perfectly integrated with a pervaporation membrane working with the same membrane area and the same reactor volume. For R = 0 the system behaves as a plug flow reactor (PFR) whose output enters the separation unit.

These outcomes are graphically depicted in Figure 10.

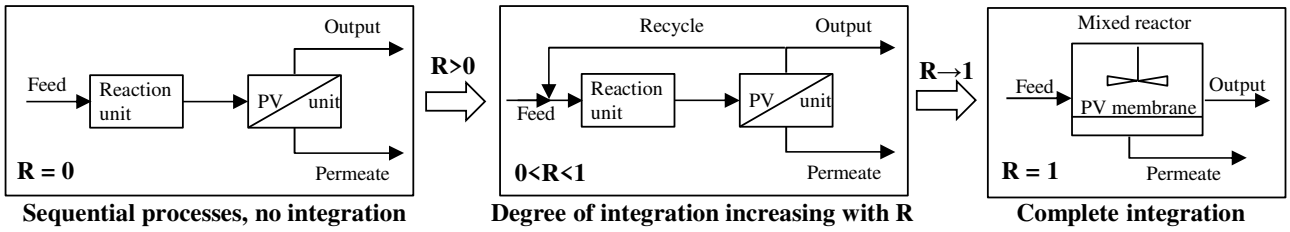

Figure 10. Processes schemes obtained at different recycle ratio.

The number N of blocks may vary from 1 to ∞. N = 1 indicates a PFR whose output enters the separation unit, thus representing the same case as R=0. On the other hand, increasing N results in a configuration where the integration of the plug flow reactors with the pervaporation units progressively increases. The situations which take place when N increases are graphically represented in Figure 11. The integration is complete when N→ ∞ and in this case the overall system behaves as a single apparatus composed by a PFR with a membrane inside.

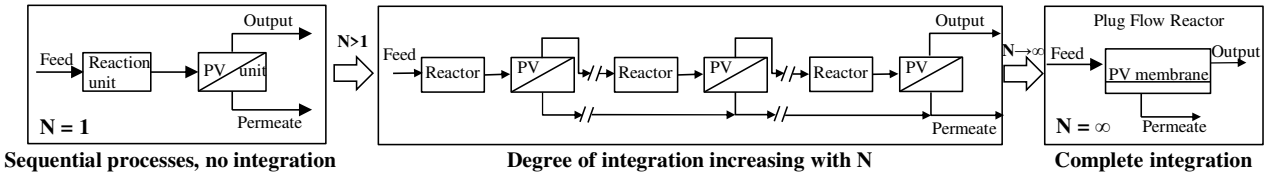

Figure 11. Processes schemes obtained at different N values.

The effects of R and N on the maximum yield have been studied by means of process simulation. Results are shown in Figure 12.

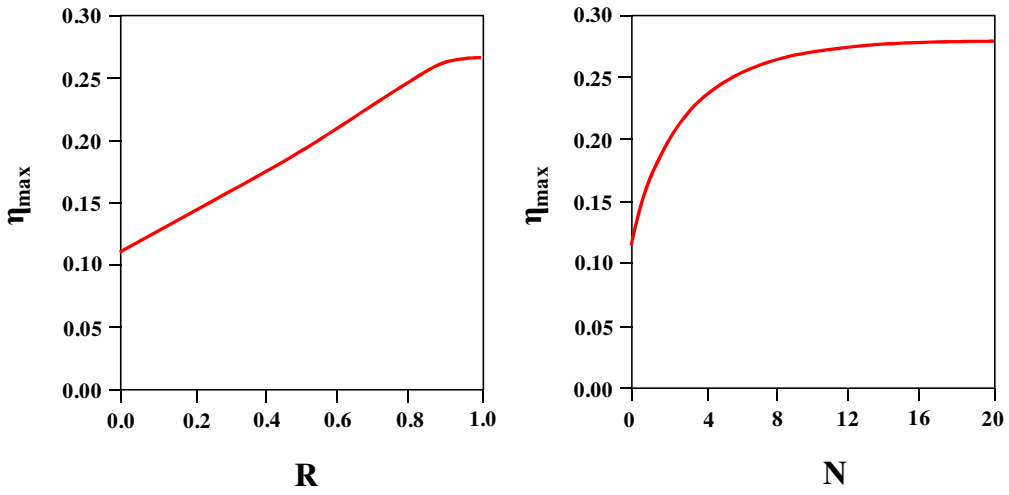

Figure 12. Profiles of the maximum yield of the process by varying R and N but maintaining the same area of the membrane and the same volume of the reactor. The curves are relative to the case 1/Pe = 0.2.

It is evident that the yield increases both with N and with R because in both cases reaction and separation become more integrated with the consequent advantages previously mentioned.

By summarizing, process intensification is the result of an appropriate choice of the reacting system and of the operating conditions.

3. High added value chemicals obtained by reduction reactions

3.1. H_2 production

Hydrogen is considered the clean fuel of the future as it can be obtained from water and converted back into water when it is oxidized without producing air pollutants or greenhouse gases. The hydrogen fuel cells may be considered as a sources of "pollution-free" energy and are now being used in buses and cars. In the chemical industry hydrogen is used for the production of ammonia, cyclohexane, and methanol, which are intermediates for the synthesis of fertilizers, plastic materials and pharmaceutical products, and also to remove sulphur from fuels during the oil-refining process. Hydrogen production is a key process for the modern society due to the absence of natural deposits. Currently, the foremost technology for its production is (i) the steam reforming of hydrocarbons, while secondary methods are (ii) thermochemical processes using heat and chemical reactions to release hydrogen from organic materials such as fossil fuels and biomass, and (iii) the splitting of water into hydrogen and oxygen by electrolysis or solar energy. The latter process is one of the most interesting and sustainable ways to achieve clean and renewable energy systems, although it is still far from being industrially exploited. Even if the first experiment of photocatalytic water splitting was reported in 1972 by Fujishima and Honda [63] the hydrogen yields obtained by using this technology are generally low. This is mainly due to fast backward reactions of H_2 to form H_2O, and to electronic (conduction and valence band position) and/or thermodynamic limitations of the used semiconductors for H_2 and O_2 evolution. In this scenario PMRs, in which the membrane divides the reactor into two compartments thus avoiding the back reaction between H_2 and O_2, can play a significant role.

In 1998 Fujihara et al. [64] performed the photochemical splitting of water under UV light in a reactor with two compartments separated by means of a Nafion® membrane and combined via platinum electrodes (Figure 13). The reduction of water to hydrogen was carried out in a solution of bromide ions containing Pt-TiO_2 particles in dispersion. The oxidation to oxygen occurred in the presence of Fe^{3+} ions and bare TiO_2. While operating, bromide ions were oxidized to bromine and H^+ ions were reduced to H_2 on the surface of TiO_2 dispersed in the first compartment. In the other compartment Fe^{3+} ions were reduced to Fe^{2+} ions and water was oxidized to oxygen by the photogenerated electrons and holes, respectively. At the electrodes Br_2 was reduced back to Br^- in the first compartment, while in the second Fe^{2+} were oxidized back to Fe^{3+} ions. Protons, passing through the membrane, preserved the electric neutrality and the pH of the solutions. A 500 W Hg lamp was used to irradiate both compartments. When the electric contact between the two compartments was interrupted, H_2 evolution was observed for a short time from the start of the irradiation and its quantity was low, due to the lack of Fe^{3+} ions in the solution. The maximum amounts of O_2 and H_2 produced were 1.3 and 2.8 $\mu mol \cdot h^{-1}$, respectively. Although the overall efficiency was reduced by the occurrence of parasitic reactions (the formation of Br_3^- and $PtBr_6^{2-}$ species was detected) this system represents one of the first innovative applications to accomplish water splitting avoiding the backward reaction between H_2 and O_2.

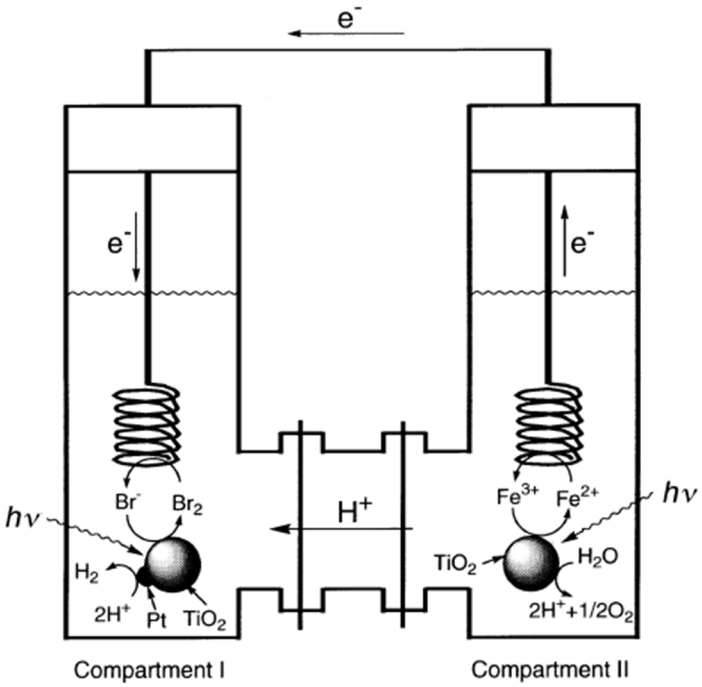

Figure 13. Schematic representation of the photo-reactor used for water splitting. Reproduced with permission from Ref. [64].

It has been seen that some catalysts were efficient toward the half reaction of water splitting but not toward the overall reaction. For this reason, systems combining different photocatalysts suitable for H_2 and O_2 evolution, respectively, have been developed. Consequently, appropriate redox mediators (Ox/Red pairs having proper potential to scavenge holes and accept electrons) have been opportunely used in order to regenerate the photocatalyst.

The main reactions occurring in the membrane reactor used by Wu and co-workers [65,66] for water splitting are reported in Figure 14. The reactor, irradiated by a 300 W-Xenon lamp, is divided in two compartments by means of a modified Nafion® membrane that allows, at the same time, the transport of protons and of the redox mediator ions (Fe^{3+}/Fe^{2+}). Pt/$SrTiO_3$:Rh was used as the photocatalyst for H_2 evolution, while WO_3 [65] or $BiVO_4$ [66] for O_2 formation. By using this configuration, water was oxidized by the photogenerated holes in one compartment producing oxygen while the photogenerated electrons reduced the Fe^{3+} ions; in the other container the photo-excited electrons reduced water to hydrogen and the holes were scavenged by the reduced form of the redox mediator (Fe^{2+}). Electrons circulated through the membrane via the redox mediator, and the mass and charge balances were preserved by the diffusion of H^+ ions through the membrane.

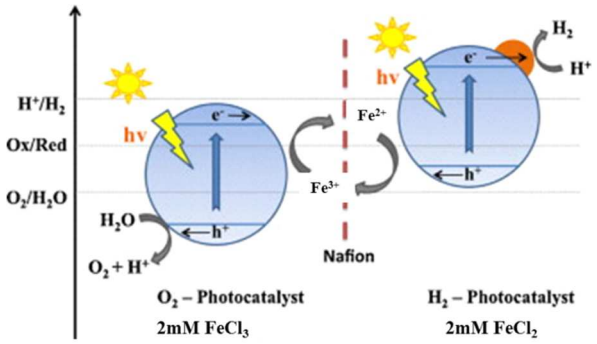

Figure 14. Schematic representation of a twin membrane reactor. Adapted with permission from Ref. [66]

Hydrogen and oxygen were obtained in stoichiometric amounts (molar ratio 2:1) demonstrating that the overall water splitting occurs in the reactor. For the sake of comparison, some runs were performed without the separating membrane in the presence of a dispersion of both the photocatalysts for hydrogen and oxygen evolution, respectively. In this case the amount of the evolved hydrogen was significantly lower than that observed in the twin reactor, thus proving that the overall efficiency decreases when the water-splitting backward reaction is not impeded (Figure 15). Hydrogen evolution rates of 1.59 and 0.65 μmol g^{-1} h^{-1} were obtained in the presence of WO_3 and $BiVO_4$ as O_2-photocatalysts, respectively.

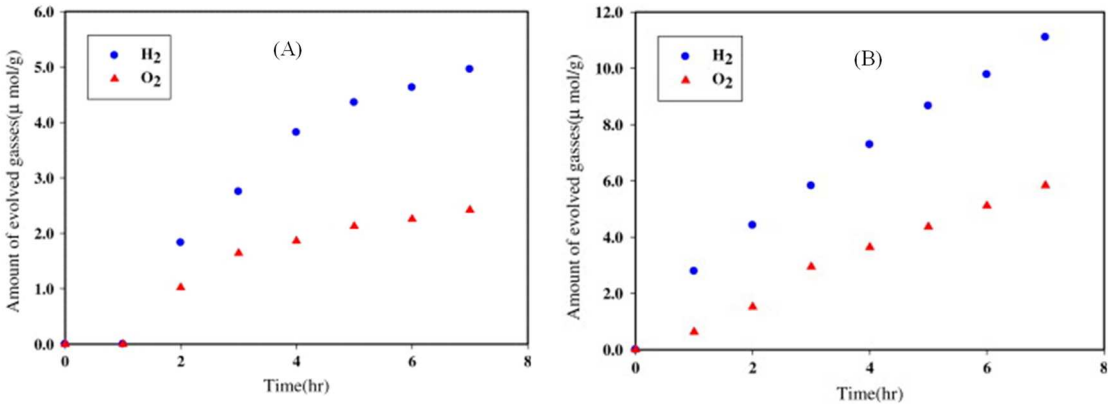

Figure 15. Time-dependence of evolved amount of H_2 and O_2 in the absence (A) and in the presence (B) of the separating membrane. Reproduced with permission from Ref. [65].

$[Co(bpy)_3]^{3+/2+}$ (2,2′-bipyridine ligands) and $[Co(phen)_3]^{3+/2+}$ (1,10-phenanthroline ligands) redox couples were used as electron mediators, in a very similar system capable to perform overall water splitting under visible light irradiation. [67] The two compartments of the reactor were separated by a membrane filter. A comparison between different pH values and various catalysts for H_2 and O_2 evolution was done and the best results were obtained at natural pH by using $SrTiO_3$:Rh and $BiVO_4$ suspended in the aqueous Co-complex solutions as the H_2 and O_2 photocatalysts, respectively. In particular $[Co(bpy)_3]^{2+}$ and $[Co(phen)_3]^{2+}$ were used as sacrificial reagents for H_2 evolution, while $[Co(bpy)_3]^{3+}$ and $[Co(phen)_3]^{3+}$ for O_2 evolution. The electron mediators $[Co(bpy)_3]^{3+/2+}$ and $[Co(phen)_3]^{3+/2+}$ worked only when $SrTiO_3$:Rh was used with $BiVO_4$ thus indicating the importance of opportunely coupling photocatalysts with suitable mediators.

In order to carry out the water splitting avoiding the contact between H_2 and O_2, Selli et al. [68] proposed a two-compartments Plexiglas reactor separated by a cation exchange membrane and a titanium electrode (Figure 16). In the side in which the water oxidation was carried out, the Ti electrode was covered by radio frequency magnetron sputtering with a TiO_2 film, consisting of pure rutile or an anatase/rutile mixture, which was irradiated with a UV or visible light lamp. Platinum was deposited on the other side of the electrode. In the two compartments of the cell, aqueous solutions of NaOH and H_2SO_4 were respectively used as the electrolytes without the addition of sacrificial agents. The highest H_2 evolution was obtained in the presence of a rutile TiO_2 active also under visible light irradiation. The photon efficiency under UV irradiation was 2.1%, while it decreased down to 0.36% by using visible light.

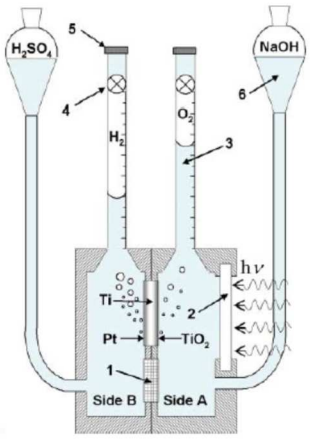

Figure 16. Schematic representation of the system reported in the reference. Reproduced with permission from Ref. [68].

A similar device, in which a dual-layer (TiO_2-WO_3) photocatalytic thin film was used as photoelectrode, showed a good water splitting efficiency under visible light irradiation [69]. Mono layer (TiO_2 or WO_3) or dual-layer (TiO_2 deposited on WO_3) films were deposited on Ti foils by radiofrequency magnetron sputtering technique at different temperatures and sputtering power, in order to found the best operating conditions. A commercial Nafion® membrane with a thickness of 178 µm (allowing only proton transfer) was used to separate the reactor in two compartments that were filled with a NaOH (oxygen side evolution) and a H_2SO_4 (hydrogen side evolution) solution. A thin layer of Pt was deposited on the photoelectrode where H_2 evolution occurred. The best configuration resulted the dual-layer film prepared at high temperature. These results can be explained by considering the higher crystallinity degree, the red shift in the light absorption of these samples and, mainly, the charge carriers separation between the two oxides which favoured the transport of photo-generated electrons and holes (as proved by means of cyclic voltammetry measurements). The amounts of H_2 and O_2 produced by the TiO_2-WO_3 film over 8 h of reaction were 38.69 and 26.24 µmoles (Photon-to-Hydrogen efficiency 0.64%) under UV light and 6.35 and 10.74 µmoles (Photon-to-Hydrogen efficiency 0.026%) under visible light irradiation.

Seger et al. [70] built a polymer membrane electrode assembly consisting of a TiO_2 photoanode, Platinum deposited on carbon black (Pt-CB) as the cathode, and a proton exchange membrane (Nafion®) to produce hydrogen from a methanol solution under UV light and with no applied bias (Figure 17). H_2 evolved with a rate of 69 µL $h^{-1}cm^{-2}$.

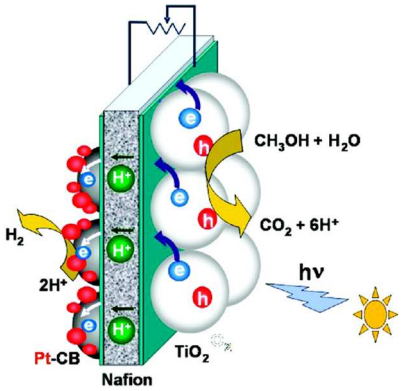

Figure 17. Scheme of the photoelectrolysis cell based based on TiO_2/Nafion/Pt assembly. Reproduced with permission from Ref. [70].

Marschall et al. [71] performed the H_2 production under solar light irradiation, without the application of an external bias and the use of electrolytes, using P25 TiO_2 as photocatalyst in a two compartments photoelectrochemical cell, in the presence of different types of composite proton exchange membranes acting as proton conductors, separators and supports for a carbon coated TiO_2 photoanode and a Pt cathode. The used proton exchange membranes were commercial Nafion® and FKE® (Fumatek) membranes, laboratory made sulfonated polyethersulfone (sPES) polymer membranes and composite membranes consisting of sPES and sulfonated mesoporous silica (Si-MCM-41) nanoparticles. Thin layers of Pt and carbon fibres were deposited on the opposite side of the membranes, and the carbon side was coated with a thin film of TiO_2. The highest hydrogen evolution rate (Figure 18) was observed in 0.01 M HCl solution by using the sulfonated polyethersulfone polymer membranes. By adding HCl the concentration of protons in the system increased, and their diffusion and mass transport to the Pt surface increased, supplying an additional driving force for the hydrogen production.

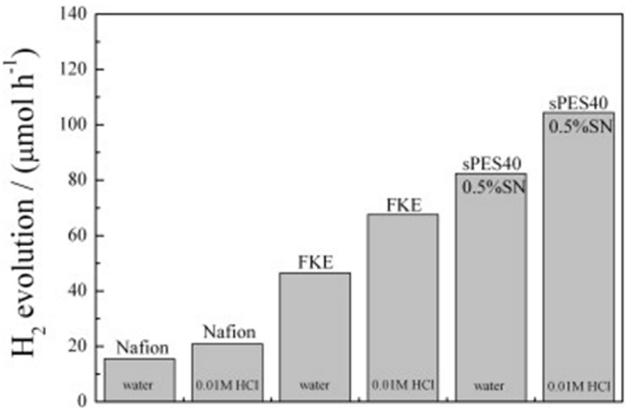

Figure 18. Hydrogen evolution rate in the presence of different membranes. Reproduced with permission from Ref. [71].

Tsydenov et al. [72] engineered a membrane photocatalytic system based on a porous polymeric membrane (PTFE -MFFK-3) impregnated with TiO_2 and a reduction (Pt) and an oxidation co-catalysts deposited on the different sides of the membrane, respectively. Different types of membranes were prepared by varying some parameters during the synthesis (TiO_2 and Pt deposition methods, TiO_2 weight and Pt concentration) and various operating configurations were tested. The photocatalytic experiments were carried out in a two chambers reactor separated by the membrane under UV light irradiation. One or both sides were filled with 6 vol.% aqueous ethanol solution. The products detected in the liquid and gas phases were CH_3COOH, CH_3CHO, CH_4, C_2H_6, CO_2 and H_2 and their distribution depended on the experimental conditions. The best results (H_2 evolution rate 15 ml/h) were obtained by using membranes with good mechanical stability, low levels of H_2 permeability, pores highly clogged by the photocatalyst and with a reactor configuration in which only a compartment was filled with the ethanol solution. Although the membrane showed high activity in hydrogen production, it was not possible to completely separate the gaseous reaction products. Successively the authors [73] tried to improve the efficiency of the system by loading the photocatalytic membrane with Nafion® in order to decrease the hydrogen permeability and to obtain a better separation of the products. The influence of Nafion® amount and ethanol concentration on the membranes permeability were investigated and the results demonstrated that, although the presence of Nafion® reduced the permeability of the membrane, the separation of the gaseous products, H_2 and CO_2, did not increase. The authors hypothesized that the H_2 evolution depended principally on the internal structure of the TiO_2 coating and, probably, Nafion® was not evenly distributed inside the TiO_2 layer.

A self-assembled functionalized phospholipid membrane was tested for the visible light photocatalytic H_2 evolution from aqueous triethanolamine (TEOA) solutions [74]. In this membrane a ruthenium based photosensitizer and a cobalt based catalyst were co-embedded. Generally, cobalt-based catalysts for H_2 generation work in organic or in mixed organic-water solvents, and it was demonstrated that the presence of water decreased the catalysts efficiency. In this paper the use of functionalized vesicles (prepared from different lipids) membranes avoided the catalyst solubility problems, while the contemporary presence of the two components into the membranes allowed a close interaction between the photosensitizer and the catalyst. No hydrogen production was observed in the absence of a single component (photosensitizer or reducing catalyst) and of electron donors (TEOA), demonstrating that all of the components were necessary. In the best conditions the amount of H_2 produced was 11.8 μmol over 13 h of irradiation.

Membranes obtained by deposition of TiO_2 and Pt/TiO_2 films on glass fibres were tested for H_2 production by photo-steam reforming of ethanol under UV light [75]. CO_2 and H_2 were the major products detected and the highest H_2 evolution rate (4 μmol h^{-1}) was measured in the presence of the membrane in which 1.5%Pt - TiO_2 film was deposited.

One of the limits of the electro-catalytic technologies for hydrogen production from water splitting is the necessity to cover the electrode with platinum as the catalyst in order to facilitate the transfer of electrons to water. Some studies reported the use of supramolecular homogeneous catalysts dissolved in the solution to transport the electrons from the electrode to the water molecules. In this way it is not necessary to plate the electrode with platinum based materials. To this aim Zamfirescu et al. [76] proposed a photochemical water splitting device consisting of two reactors divided by a Nafion® proton conducting membrane (Figure 19) and in which supramolecular complexes based on ruthenium-$(bipyridine)_3^{2+}$ photosensitizers were dissolved. The supramolecular system contains the photo-sensitizers, electron acceptors and donors, the active catalytic centres and pH regulators. In fact, no external bias was applied to the different membrane sides and the driving force to proton transport along the membrane is supplied by a H^+ concentration gradient (pH = 7.2 in the oxidation reactor and pH = 9.1 in the reduction reactor). Both reactors were irradiated with solar light and the supramolecular systems were capable of generating electrons or holes under irradiation without being consumed. Moreover, the appropriate catalyst used for water reduction was able to increase the life time of the photoelectrons, enhancing the H_2 evolution efficiency. Even if the efficiency of this system is low, this can be compensated by the low cost of the used chemicals and of the electrodes.

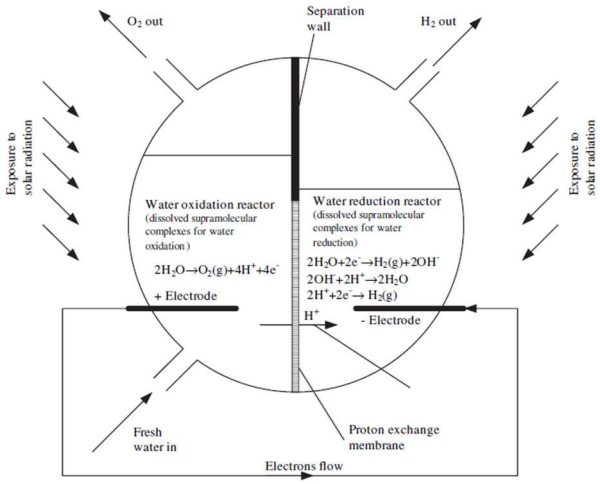

Figure 19. Scheme of the water splitting reactor used by Zamfirescu. Reproduced with permission from Ref. [76].

In most of the above mentioned examples the use of sacrificial electron or hole scavengers is reported. Generally, scavengers are used to prevent photocorrosion of some semiconductors which is not the case of TiO_2 which is stable in water under irradiation. Therefore, in the presence of TiO_2 their use is due to the fact that typically water oxidation is slower than water reduction thus becoming the rate limiting step [77]. In fact, in many reports researchers focus on hydrogen production by scavenging holes with strong reducing agents [78]. However, the use of scavengers implies a reduction in the stored energy which can be even zero when strong reducing agents are used. The energy stored in the new chemical bonds formed is thermodynamically equal to the difference between the redox potential of the reduction and oxidation half-reactions (hydrogen and oxygen formation, respectively) [79]. In the presence of scavengers the stored energy is accordingly decreased by the difference between the redox level of the electron or hole scavenger and the water oxidation or reduction, respectively. Therefore, the system becomes energetically down-hill and even a direct reduction of water by the sacrificial agent is possible [80]. Even if such studies are of great value in development and optimization of new catalysts for specific half-reactions, long-term sustainable solutions have to involve full water splitting to H_2 and O_2.

3.2. CO_2 reduction

The high level of CO_2 present in the atmosphere has become a global environmental issue because it contributes to the increase of global temperature and to climate changes due to the "greenhouse effect". Therefore, scientists devoted increasing attention to control CO_2 emissions and to develop efficient CO_2 capture and utilization systems, in particular to convert CO_2 into useful chemical species and fuels. In this context, CO_2 solar energy conversion by artificial photosynthesis represents an important research area. Many studies have been carried out in the last years on CO_2 reduction by using TiO_2 as the photocatalyst [81-85], but the main drawbacks of this processes are the low photoconversion efficiency due to thermodynamic limitations, and the occurrence of decomposition of the obtained products (like methanol, formic acid, formaldehyde) due to the higher reactivity of these compounds with respect to CO_2. The use of a membrane reactor where the photocatalyst is immobilized into a polymeric membrane can be an interesting and valid solution to be adopted. Indeed, this allows the control of the contact time between the catalyst and the species in the solution, and the recovery of the catalyst.

Ichikawa and Doi [85] reported the hydrogen production with the simultaneous CO_2 conversion under UV light irradiation in a single unit photoelectrocatalysis system. This consisted of a thin TiO_2 film as the photocatalyst for H_2 generation, an electrocatalyst containing zinc oxide and copper, and a Nafion® film as proton separator (Figure 20). Methane, ethylene and H_2 were the foremost products observed in the gas phase, while traces of formic acid and ethanol were present in the solution. A good activity and selectivity toward the gaseous products was obtained by operating under a pulsed bias between the photocatalyst and the electrocatalyst.

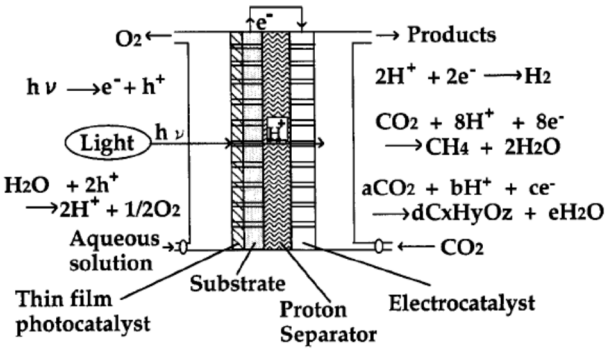

Figure 20. Single unit photoelectrocatalysis system. Reproduced with permission from Ref. [85].

Premkumar and Ramaraj [86] used metal porphyrins (MP) and phthalocyanines (MPC) adsorbed on Nafion® membrane systems to carry out the photocatalytic reduction of carbon dioxide in liquid phase by using triethanolamine as sacrificial electron donor and scavenger for the holes. Formic acid was obtained as reduction CO_2 product with a high turnover number. MPs and MPCs interacted each other and with the units of the membrane thus forming a three-dimensional disordered network very active in the charge separation.

A good photocatalytic conversion of CO_2 was realized by using nanoscale Degussa P25 TiO_2 (TiO_2 loadings about 10 wt%) particles homogeneously dispersed in porous cavities of Nafion® membrane films [87]. The reaction was carried out in liquid CO_2 in a high-pressure reactor equipped with two quartz windows (Figure 21), using a xenon arc lamp as irradiation source. The obtained products under these conditions were formic acid, methanol and acetic acid, and their amounts increased by increasing the number of deposition steps of the TiO_2 film onto the membrane. In the presence of a single TiO_2-loaded Nafion® film the products amount was 190 μmol/g for formic acid, 280 μmol/g for methanol and 30 μmol/g for acetic acid. A lower amount of formic acid and traces of methanol were measured by using TiO_2 as powder suspended in liquid CO_2. These results demonstrated the positive effect of the catalyst immobilization in a solid matrix that avoids the problems due to the aggregation of the particles.

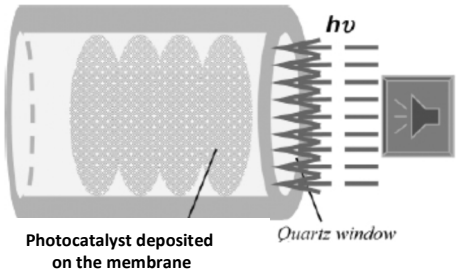

Figure 21. Experimental setup for the photoreduction of liquid CO_2 with TiO_2- loaded Nafion® films as photocatalyst. Reproduced with permission from Ref. [87].

Successively the same authors coated the membrane film containing TiO_2 with silver metal in order to improve the CO_2 conversion [88]. In this case, by working under the identical experimental conditions of the previous work [87], the main product was methanol instead of formic acid and the CO_2 conversion was higher (Figure 22). The enhancement in the photoactivity was attributed to the better separation charge of TiO_2 in the presence of Ag and a very low CO_2 amount was measured using the Nafion® membrane films containing only silver nanoparticles.

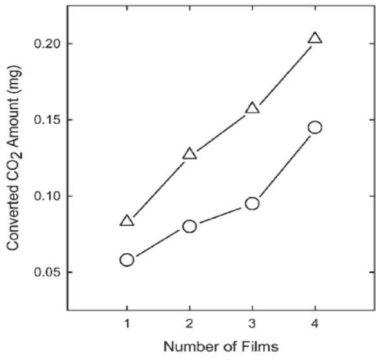

Figure 22. CO_2 conversion as a function of the number of stacked catalytic films with (△) and without (○) the silver coating of the embedded TiO_2 nanoparticles. Reproduced with permission from Ref. [88].

Photocatalytic gas phase reduction of CO_2 and water vapour to hydrocarbons under sunlight irradiation was performed in the presence of thin wafers of TiO_2 (Degussa P25) sputtered with Cu and/or Pt nanoparticles. The effect of the relative humidity, the exposure time and the use of nanoporous TiO_2 pellet acting as a flow-through membrane was investigated [89]. Methane, hydrogen and carbon monoxide were the main products; the contemporary presence of both Cu and Pt on the wafer surface enhanced the reaction rate and the highest productivity was obtained with relative humidity of 55%. Moreover, ca. 25% increase in the reduction products amount was observed when the system was used in a flow-through membrane implementation, due to removal of the products from the surface of the catalyst, which avoided their re-oxidation.

Cheng et al. [90] used an optofluidic two chambers membrane microreactor with a high surface area/volume ratio with the aim to improve the light distribution inside the reactor and the proton transfer, and to increase the specific surface area. The composite membrane consisted of a carbon paper coated on one side with Degussa P25 TiO_2 (Figure 23) and on the other side made hydrophobic by a treatment with poly-tetrafluoroethylene (PTFE), in order to separate the gas/liquid phases and to prevent water leakages. The reaction was carried out under UV light irradiation and only the methanol yield was measured to evaluate the performance of the reactor by varying the operative parameters (water flow rate, light intensity, catalyst loading). A maximum methanol yield of 111.0 µmole/g-cat h was achieved at a flow rate of 25 µL/min and under a light intensity of 8 mW/cm^2 and a catalyst loading of 4.5 mg/cm^2.

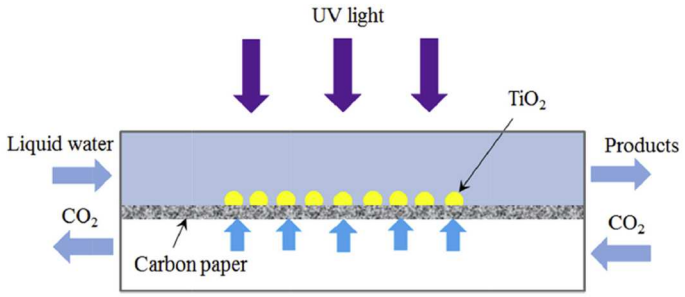

Figure 23. Scheme of of the optofluidic membrane microreactor for the photocatalytic reduction of CO_2. Reproduced with permission from Ref. [90].

Sellaro *et al.* [91] performed the photocatalytic CO_2 reduction, under mild experimental conditions, in a continuous photocatalytic membrane reactor in which laboratory made TiO_2 was immobilized in Nafion® membranes, synthesized in different conditions and used in various configurations. A good catalyst distribution inside the membrane was obtained by using an appropriate co-solvent (e.g. ethanol) for the preparation of the polymeric solution and an appropriate TiO_2 amount (ca. 1.2 wt%). The runs were carried out under UV light in liquid phase using H_2O as the reducing agent, by placing the membranes into a flat sheet membrane module equipped with a quartz window allowing the irradiation. By working in continuous mode, H_2O:CO_2 stream with a molar ratio equal to 5:1 was alimented in the reaction chamber at room temperature and the trans-membrane pressure difference was set at 2 bar. The membrane showed a good permeance of CO_2, and this, coupled with the presence of hydrophilic domains, allowed the access of the reagents inside. The main photoreduction product was methanol and using the membrane with the best TiO_2 distribution the MeOH flow rate/catalyst weight was 45 µmol $g_{catalyst}^{-1}$ h^{-1}. In this case the use of membranes with photocatalyst embedded inside and a continuous flow mode allowed to remove methanol from the reactor volume avoiding its over oxidation. Although CO_2 conversion and methanol yield were low, they are among the highest reported in the literature to-date. In a successive work [92] authors used exfoliated C_3N_4 instead of TiO_2 in a similar system configuration. In this case the membrane reactor converted at least 10 times more carbon than the batch system, as a result of the continuous operation

mode and of the improved dispersion of catalyst once embedded in the Nafion® matrix. In the presence of C_3N_4, CO_2 was converted in a different set of products compared to the system with TiO_2, i.e. methanol, ethanol, formaldehyde and acetone. The product distribution strongly depended on H_2O/CO_2 feed molar ratio and residence time. Notably, this work for the first time highlights the need of a synergistic approach connecting process parameters and product distribution, conversion and selectivity for CO_2 photoreduction.

One of the problems of CO_2 reduction in aqueous solutions is the low quantum efficiency due to preferential H_2 formation as this is a less difficult reaction from the thermodynamic point of view. The use in the same system of two catalysts, one more suitable for the CO_2 reduction and the other for H_2O oxidation, can improve the selectivity toward the CO_2 reduction compounds. Sato et al. [93] performed the CO_2 photo-reduction in water solution by using as reduction system a hybrid photocatalyst constisting of a semiconductor photosensitizer coated with a metal complex electrocatalyst (InP/RuCP) and Pt/TiO_2 (P25) as oxidation photocatalyst, in a two compartment quartz cell separated by a proton exchange membrane (Nafion®), under simulated solar light irradiation. By selecting the two photocatalysts in appropriate manner (in term of positions of the edge of the bands) it was possible to realize the so-called Z-scheme (or two-step photoexcitation) and the electron transfer from the photoanode to the photocathode without the application of an external bias. Formic acid was the main reduction product and the highest current efficiency was > 70% in an aqueous 10 mM solution of $NaHCO_3$. It was proved by isotopic labelling that H_2O and CO_2 provided the carbon and hydrogen atoms for formate formation, in accord to the reactions (10) and (11), confirming the effective reduction of CO_2 and the absence of organic residues on the catalyst surface. In this case, H_2O worked as electron donor and proton source. Small amounts of H_2 and CO were also detected. The results were reproducible, however the conversion efficiency of the solar energy to chemical energy was not high (0.03%).

$$H_2O \xrightarrow{\text{catalyst, h}\nu} 0.5\ O_2 + 2H^+ + 2e^- \qquad (10)$$

$$CO_2 + 2H^+ + 2e^- \xrightarrow{\text{catalyst, h}\nu} HCOOH \qquad (11)$$

Successively, solar CO_2 photoreduction was attained in the same reactor substituting the oxidation photocatalyst with a reduced $SrTiO_3$ system [94]. The experimental set-up is represented in Figure 24. This semiconductor has the same TiO_2 band-gap but a more negative potential of the conduction band minimum. In this way the electron transfer from the conduction band of the photoanode to the valence band of the photocathode was facilitated and the conversion efficiency was improved from 0.03 to 0.14% (ca. half than that of the plants). Moreover it was observed that, unlike what seen for TiO_2, a negligible amount of formate was degraded in the presence of $SrTiO_3$ and water is preferentially oxidised to oxygen. In this case, as the re-oxidation of the obtained formate could not take place, it was possible to carry out the solar CO_2 reduction also in a single compartment reactor without membrane, achieving a solar conversion efficiency of 0.08%.

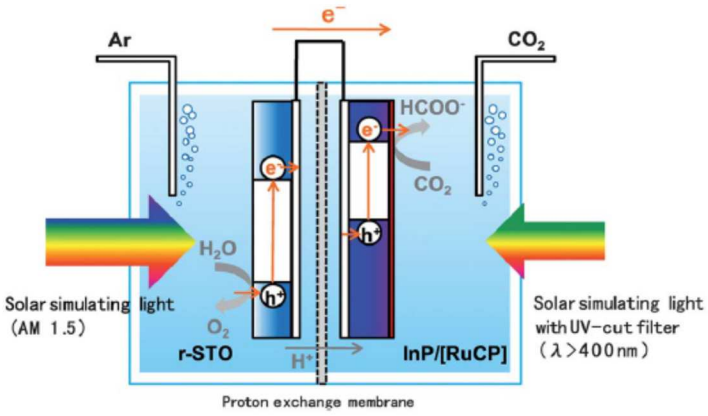

Figure 24. Schematization of the two-electrode system used by Arai et. al. Reproduced with permission from Ref. [94].

Lee et co-workers [95] performed the CO_2 hydrogenation under simulated sun light in the same twin reactor used for H_2 production [65] by adding an appropriate catalyst for CO_2 reduction in the reduction cell. In this system the H_2 produced by water splitting was used to hydrogenate the CO_2 reproducing the natural photosynthesis. First, Pt loaded $CuAlGaO_4$ was used both for H_2 generation and CO_2 reduction studying the influence of Pt loading. Hydrogen, methanol and CO were the main products and the best results were obtained with the sample Pt(1.0 wt%)/$CuGaAlO_4$ (Figure 25). Then the runs were carried out in the twin reactor where two photocatalysts were employed in the reduction cell, Pt(1.0 wt%)/$CuAlGaO_4$ for CO_2 reduction and Pt(0.8wt%)/$SrTiO_3$:Rh for H_2 production, and WO_3 in the other compartment as O_2 generating photocatalyst. The photoreduction quantum efficiency was 0.0051%, more than double than that obtained in the single system. This enhancement was attributed to the specificity of the

used photocatalysts toward the two reactions, in particular Pt(0.8 wt%)/$SrTiO_3$:Rh was a better photocatalyst than Pt(1.0 wt%)/$CuGaAlO_4$ for H_2 evolution. Furthermore, the greater H_2 yield, in turn, improved the CO_2 hydrogenation to methanol.

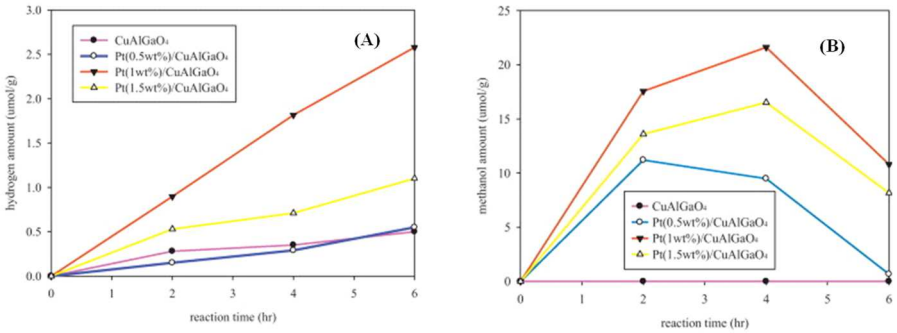

Figure 25. Hydrogen (A) and methanol (B) amount obtained by using Pt/$CuAlGaO_4$ as reduction photocatalyst. Reproduced with permission from Ref. [95].

To further enhance the photoreduction quantum efficiency of this system, a gaseous mixture of CO/CO_2 was co-fed in the twin reactor and the results were compared with those obtained when only CO or only CO_2 was used [96]. Methanol was not formed feeding only CO, probably due to the poisoning of Pt surface by the absorbed CO; moreover H_2 and O_2 evolved with an initial ratio higher than 2 owing to the simultaneous gas shift reaction ($CO + H_2O \rightarrow CO_2 + H_2$). O_2, H_2 and CH_3OH with a yield of 0.76, 0.12 and 0.52 μmol g^{-1} h^{-1}, respectively, were observed in the presence of pure CO_2. In this case the H_2/O_2 ratio was lower than two, indicating that hydrogen was consumed for the hydrogenation of CO_2 to methanol. Moreover, the CH_3OH yield was constant, suggesting that simultaneously it was formed and converted to 2-carbon compounds (for example acetaldehyde) or re-oxidized. By co-feeding CO and CO_2, the amounts of O_2, H_2 and CH_3OH were higher than those measured by using pure CO_2 and traces of methyl formate and acetaldehyde were also observed (Figure 26).

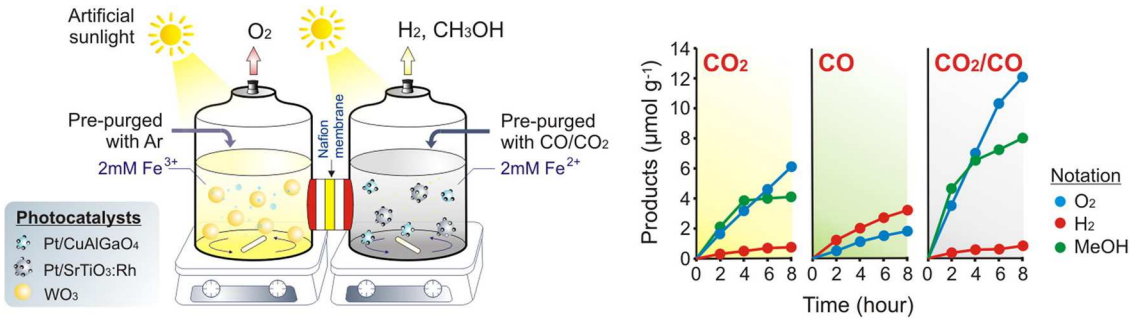

Figure 26. Twin reactor system and products obtained during the CO_2 photoreduction in the different operating condition studied by Chen et al. Reproduced with permission from Ref. [96].

In the presence of high amounts of CO, the methanol yield decreased and increased the concentration of co-products. Successively, a computational model was developed to study the influence of the operating conditions (pressure, temperature, sun light intensity, CO/CO_2 ratio) on the CO_2 reduction in the twin reactor [97]. By using the results obtained in the previous work [96] it was possible to verify the reliability of the numerical simulations. Depending on the CO_2/CO ratio, reaction temperature and pressure, different amounts of CH_3OH, $HCOOCH_3$ and CH_3CHO were obtained. The CH_3OH amount varied with the sun light intensity and increased by increasing the temperature and the pressure. The maximum production rates calculated by using a CO/CO_2 ratio of 1:2 were of 0.98, 0.1875 and 0.05 μmol g^{-1} h^{-1}, for CH_3OH, $HCOOCH_3$ and CH_3CHO, respectively, within 8 h. A good agreement was found between the experimental data and those of the model, as reported in the Figure 27.

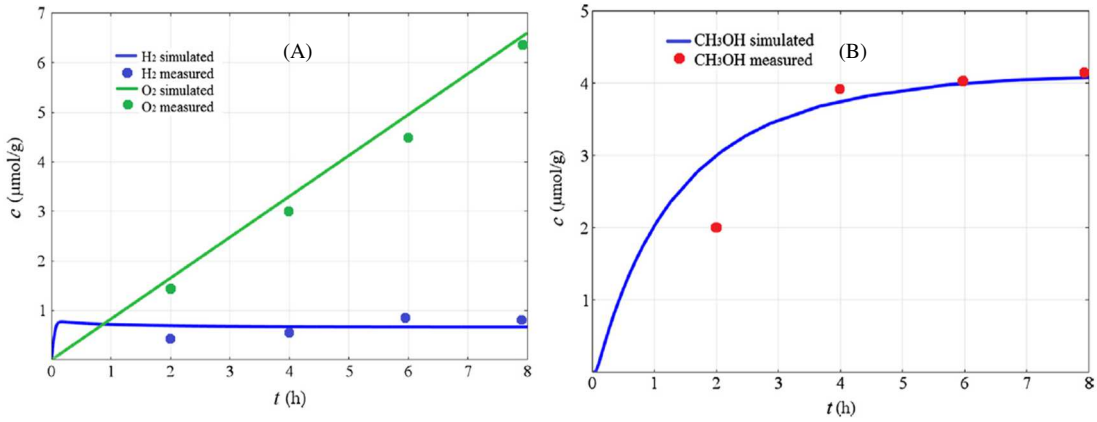

Figure 27. Hydrogen, oxygen (A) and methanol (B) production during photocatalytic reduction of pure CO_2. Reproduced with permission from Ref. [97].

3.3. Photocatalytic reduction of acetophenone to phenylethanol

Phenylethanol is a valuable compound used as a building block for the synthesis of agrochemicals, pharmaceuticals, and natural products. Phenylethanol may be extracted from natural raw feedstokes but the production process is very expensive and time demanding. Furthermore its use as a rose-like fragrance in food, beverages and personal care products [98] justifies the scientific efforts of the last decades for new, green and cheap synthetic routes. The photocatalytic hydrogenation of acetophenone has been proposed by Molinari et al. [99] as a promising green synthesis of phenylethanol. Authors used water as the solvent, UV light irradiation, commercial TiO_2 as the photocatalyst and formic acid as hydrogen and electron donor [100,101]. The reaction, carried out in the absence of oxygen, may be expressed as in Eq. 12.

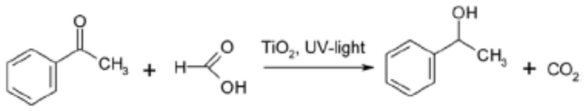

(12)

The same reaction has been also successfully carried out under visible light irradiation by doping TiO_2 with palladium by means of a deposition precipitation method.

The same authors integrated the acetophenone reduction in a PMR similar to that shown in Figure 1. The reacting mixture, irradiated in an annular Pyrex reactor (volume = 500 mL) by means of an immersed lamp and continuously purged with argon, circulated by means of a peristaltic pump also in the first compartment of the separation module. The latter is separated from a second compartment containing an organic extracting phase mechanically stirred by a motor, by a flat sheet polypropylene membrane with an exposed membrane surface area of 28.3 cm^2. Both the reaction and separation modules have been maintained at the same temperature by means of a thermostatic bath. The phenylethanol produced in the aqueous reacting phase diffused through the membrane and then dissolved into the organic extracting phase, where it was protected from successive over-hydrogenation. The integrated system showed better conversion, selectivity, yield and overall produced amount of phenylethanol than the sole photocatalytic system.

The influence of different substrate feeding mode and of different flow rates has been investigated in order to improve phenylethanol productivity.

Adding acetophenone to the reacting mixture directly drop by drop did not significantly enhance the efficiency of the process. The reactant has been also dissolved in n-heptane as the extracting phase so that it could reach the reacting zone by permeation through the membrane. Although n-heptane was completely rejected by the membrane, the final organic phase was mainly constituted by three components (n-heptane, acetophenone and phenylethanol) so that further costs for subsequent separation must be taken into account. The best feeding solution was to consider acetophenone both as reactant and organic extracting phase. This made easier the subsequent product recovery and allowed longer irradiation times as acetophenone is less volatile than n-heptane (boiling point 202 °C versus 98–99 °C).

Doping commercial TiO_2 with Pd allowed to carry out the reaction under visible light irradiation. In this system five times higher productivity of phenylethanol were obtained with respect to the bare sample irradiated with UV light.

3.4. Reduction of nitrite to ammonia

Nitrite ions are among the major causes of water pollution and their reduction is of great importance in the remediation of waste water and in the fixation of nitrogen into valuable compounds. The excessive presence of nitrite ions in drinking water is harmful to the human body and even fatal for children under 6 months of age. The reduction of nitrite to ammonia, mimicking the nitrogen fixation system by green plants, represents an interesting approach as an increasing demand for NH_3 is forecasted. Different techniques were used to this purpose and the papers on the photocatalytic reduction of nitrite are not numerous. Pandikumar et al. [102] embedded TiO_2–Au nanoparticles ((TiO_2–Au)nps) in a methyl functionalized silicate sol–gel (MTMOS) and Nafion® matrices to perform the photocatalytic reduction of nitrite to ammonia in the presence of oxalic acid as the hole scavenger. The results demonstrated the effective interfacial charge transfer process in the presence of Au and photocatalytic activity increased with increasing amounts of Au nanoparticles on TiO_2. The highest ammonia production was measured with the Nafion(TiO_2–Au)nps photocatalyst due the contemporaneous presence of Au, that accumulates electrons enhancing the charge separation, and the porous structure of the Nafion® polymeric matrix. When the same photocatalyst was used in colloidal form, indeed, a lower amount of NH_3 was obtained. The lower efficiency found by using the MTMOS/(TiO_2–Au)nps film was ascribed to the larger particles formed in the silicate sol–gel film with respect to the Nafion/(TiO_2–Au)nps film.

4. Conclusions

This review presents some heterogeneous photocatalytic reactions for the synthesis of high value added compounds carried out in photocatalytic membrane reactors. As evidenced throughout the text, the advantages of coupling photocatalytic and membrane technologies for synthetic purposes are remarkable. In fact, higher yields with respect to the sole photocatalysis can be obtained in the integrated process and both separation of the target compounds and of the photocatalyst particles is enabled in continuous, without additional post-process steps. The two technologies can be easily coupled because they work in similar operating conditions and it is possible to work modularly and with easy control of the process. The advantages of PMRs have been highlighted for some organic syntheses, but they are even more evident for reactions occurring with less efficiency such as CO_2 reduction and water splitting. In both cases has been evidenced how the control of process parameters is a key factor along with the optimization of the physico-chemical features of the photocatalysts in order to maximize the performance of the process and to address the reaction towards the desired target compounds. Unfortunately, the number of reactions carried out in PMRs in literature is still rare. For instance the synthesis of phenol from benzene, the partial oxidation of aromatic alcohols to the corresponding aldehydes and the synthesis of vanillin, CO_2 reduction, H_2 production, nitrite reduction, and the synthesis of phenylethanol have been reviewed as photocatalytic reactions carried out in PMRs. Engineering and design features of the processes, which are essential to evaluate their economic convenience towards real applications, have been only rarely investigated with some exceptions. Hopefully, the pioneering studies hereby presented could inspire researchers to further investigate the potential of photocatalytic membrane reactors for chemical syntheses by exploiting also the solar light.

References

1. M. Bellardita, V. Loddo, A. Mele, W. Panzeri, F. Parrino, I. Pibiri, L. Palmisano, Photocatalysis in dimethyl carbonate green solvent: degradation and partial oxidation of phenanthrene on supported TiO_2, RSC Adv. 4 (2014) 40859-40864.

2. S. Higashida, A. Harada, R. Kawakatsu, N. Fujiwara, M. Matsumura, Synthesis of a coumarin compound from phenanthrene by a TiO_2-photocatalyzed reaction, Chem. Commun. (2006) 2804-2806.

3. R. Ciriminna, F. Parrino, C. De Pasquale, L. Palmisano, M. Pagliaro, Photocatalytic partial oxidation of limonene to 1,2 limonene oxide, Chem. Commun. 54 (2018) 1008-1011.

4. H. Yoshida, H. Yuzawa, M. Aoki, K. Otake, H. Itoh, T. Hattori, Photocatalytic hydroxylation of aromatic ring by using water as an oxidant, Chem. Commun. (2008) 4634-4636.

5. A. Di Paola, M. Bellardita, B. Megna, F. Parrino, L. Palmisano, Photocatalytic oxidation of trans-ferulic acid to vanillin on TiO_2 and WO_3-loaded TiO_2 catalysts, Cat. Today, 252 (2015) 195–200.

6. X. Lang, H. Ji, C. Chen, W. Ma, J. Zhao, Formation of Imines by Aerobic Photocatalytic Oxidation of Amines on TiO_2, Angew. Chemie Int. Ed. 50 (2011) 3934-3937.

7. C. Guarisco, G. Palmisano, G. Calogero, R. Ciriminna, G. Di Marco, V. Loddo, M. Pagliaro, F. Parrino, Visible-light driven oxidation of gaseous aliphatic alcohols to the corresponding carbonyls via TiO_2 sensitized by a perylene derivative, Environ. Sci. Pollut. Res. Int. 21 (2014) 11135–11141.

8. M. Bellardita, V. Loddo, G. Palmisano, I. Pibiri, L. Palmisano, V. Augugliaro, Photocatalytic green synthesis of piperonal in aqueous TiO_2 suspension, Appl. Catal. B 144 (2014) 607- 613.

9. C. Pruden, J. Pross, Y. Li, Photoinduced reduction of aldehydes on titanium dioxide, *J. Org. Chem.* 57 (1992) 5087-5091.

10. M. Bellardita, A. Di Paola, E. García-López, V. Loddo, G. Marcì, L. Palmisano, Photocatalytic CO_2 Reduction in Gas-Solid Regime in the Presence of Bare, SiO_2 Supported or Cu-Loaded TiO_2 Samples, Curr. Org. Chem. 17 (2013) 2440-2448.

11. K. Park, H. Joo, K. Ahn, K. Jun, One step synthesis of 4-ethoxy-1,2,3,4-tetrahydroquinoline from nitroarene and ethanol: A TiO_2 mediated photocatalytic reaction, Tetrahedron Lett. 36 (1995) 5943-5946.

12. H. Pehlivanugullari, E. Sumer, H. Kisch, Semiconductor photocatalysis type B: synthesis of unsaturated α-cyano-homoallylamines from imines and olefins photocatalysed by silica- and cellulose-supported cadmium sulphide, Res. Chem. Intermediat. 33 (2007) 297-309.

13. L. Cermenati, C. Richter, A. Albini, Solar light induced carbon–carbon bond formation via TiO_2 photocatalysis, Chem. Commun. (1998) 805-806.

14. M. Bellardita, E. García-López, G. Marcì, L. Palmisano, Photocatalytic formation of H_2 and value-added chemicals in aqueous glucose (Pt)-TiO_2 suspension, Int. J. Hydrogen Energ. 41 (2016) 5934–5947.

15. A. Hakki, R. Dillert, D. Bahnemann, Photocatalytic conversion of nitroaromatic compounds in the presence of TiO_2, Cat. Today 144 (2009) 154-159.

16. F. Parrino, A. Di Paola, V. Loddo, I. Pibiri, M. Bellardita, L. Palmisano, Photochemical and photocatalytic isomerization of trans-caffeic acid and cyclization of cis-caffeic acid to esculetin, Appl. Catal. B 182 (2016) 347–355.

17. N. Zeug, J. Bücheler, H. Kisch, Catalytic formation of hydrogen and carbon-carbon bonds on illuminated zinc sulfide generated from zinc dithiolenes, J. Am. Chem. Soc. 107 (1985) 1459-1465.

18. B. Ohtani, H. Osaki, S. Nishimoto, T. Kagiya, A redox combined photocatalysis: New method of N-alkylation of ammonia by TiO_2/Pt suspended in alcohols, Tetrahedron Lett. 27 (1986) 2019-2022.

19. P. T. Anastas, J. C. Warner, Green Chemistry: Theory and Practice, Oxford, University Press, New York 2000.

20. R. Molinari, C. Lavorato, T. Poerio, Performance of vanadium based catalyst in a membrane contactor for the benzene hydroxylation to phenol, Appl. Catal. A 417 (2012) 87–92.

21. Y. Liu, K. Murata, M. Inaba, Direct oxidation of benzene to phenol by molecular oxygen over catalytic systems containing $Pd(OAc)_2$ and heteropolyacid immobilized on HMS or PIM, J. Mol. Catal. A Chem. 256 (2006) 247–255.

22. R. Molinari, P. Argurio, T. Poerio, Vanadyl acetylacetonate filled PVDF membranes as the core of a liquid phase continuous process for pure phenol production from benzene, J. Membr. Sci. 476 (2015) 490–499.

23. S. Niwa, M. Eswaramoorthy, J. Nair, A. Raj, N. Itoh, H. Shoji, T. Namba, F.Mizuka, A one-step conversion of benzene to phenol with a palladium membrane, Science 295 (2002) 105–107.

24. D. Bianchi, L. Balducci, R. Bortolo, R. D'Aloisio, M. Ricci, G. Span, R. Tassinari,C. Tonini, R. Ungarelli, Oxidation of benzene to phenol with hydrogen peroxide catalyzed by a modified titanium silicalite (TS-1B), Adv. Synth. Catal. 349 (2007) 979–986.

25. R. Molinari, T. Poerio, Remarks on studies for direct production of phenol in conventional and membrane reactors, Asia-Pac. J. Chem. Eng. 5 (2010) 191–206.

26. N. Itoh, S. Niwa, F. Mizukami, T. Lnoue, A. Igarashi, T. Namba, Catalytic palladium membrane for reductive oxidation of benzene to phenol, Catal. Commun. 4 (2003) 243–246.

27. W. Laufer, W.F. Hoelderich, New direct hydroxylation of benzene with oxygen in the presence of hydrogen over bifunctional ion-exchange resins, Chem. Commun. (2002) 1684–1685.

28. D. Bianchi, R. Bortolo, R. Tassinari, M. Ricci, R. Vignola, A novel iron-based catalyst for the biphasic oxidation of benzene to phenol with hydrogen peroxide, Angew. Chem. Int. Ed.39 (2000) 4321–4323.

29. X.B. Wang, Y. Guo, X.F. Zhang, H. Liu, J. Wang, K.L. Yeung, Catalytic properties of benzene hydroxylation by TS-1 film reactor and Pd-TS-1 composite membrane reactor, Catal. Today 156 (2010) 288–294.

30. R. Molinari, A. Caruso, T. Poerio, Direct benzene conversion to phenol in a hybrid photocatalytic membrane reactor, Catal. Today 144 (2009) 81–86.

31. A. Noubigh, A. Mgaidi, M. Abderrabba, E. Provost, W. J. Fürst, Effect of salts on the solubility of phenolic compounds: experimental measurements and modelling, J. Sci. Food. Agric. 87 (2007) 783-788.

32. V. Brezova, A. Blazkova, E. Borosova, M. Ceppan, R. Fiala, The influence of dissolved metal ions on the photocatalytic degradation of phenol in aqueous TiO_2 suspensions, J. Mol. Catal. A 98 (1995) 109-116.

33. I.K. Konstantinou, T.A. Albanis, TiO_2-assisted photocatalytic degradation of azo dyes in aqueous solution: kinetic and mechanistic investigations – a review, Appl. Catal. B 49 (2004) 1-14.

34. T. Mallat, A. Baiker, Oxidation of alcohols with molecular oxygen on solid catalysts, Chem. Rev. 104 (2004) 3037– 3058.

35. G. Palmisano, V. Augugliaro, M. Pagliaro, L. Palmisano, Photocatalysis: a promising route for 21st century organic chemistry Chem. Commun. (2007) 3425–3437.

36. S. Yurdakal, G. Palmisano, V. Loddo, V. Augugliaro, L. Palmisano, Nanostructured rutile TiO_2 for selective photocatalytic oxidation of aromatic alcohols to aldehydes in water, J. Am. Chem. Soc. 130 (2008) 1568-1569.

37. A. Abd-Elaal, F. Parrino, R. Ciriminna, V. Loddo, L. Palmisano, M. Pagliaro, Alcohol-selective oxidation in water under mild conditions via a novel approach to hybrid composite photocatalysts, Chem. Open 4 (2015) 779 – 785.
38. G. Camera-Roda, F. Santarelli, V. Augugliaro, V. Loddo, G. Palmisano, L. Palmisano, S. Yurdakal, Photocatalytic process intensification by coupling with pervaporation, Catal. Today 161 (2011) 209-213.
39. G. Camera Roda, V. Augugliaro, V. Loddo, G. Palmisano, L. Palmisano, Production of aldehydes by oxidation in aqueous medium with selective recovery of the product by means of pervaporation, US patent: US08884069.
40. K.W. Böddeker, Terminology in pervaporation J. Membr. Sci. 51 (1990) 259-272.
41. A.K. Sinha, U.K. Sharma, N. Sharma, A comprehensive review on vanilla flavor: extraction, isolation and quantification of vanillin and others constituents, Int. J. Food Sci. Nutr. 59 (2008) 299–326.
42. N.J. Walton, M.J. Mayer, A. Narbad, Vanillin, Phytochemistry 63 (2003) 505–515.
43. H. Korthou, R. Verpoorte, Vanilla, in: R.G. Berger (Ed.), Flavours and Fragrances, Springer-Verlag, Berlin, Heidelberg, pp. 203–217, 2007.
44. M.M. Bomgardner, The problem with Vanilla, C&EN 94 (2016) 38-42.
45. J. Pickett-Baker, R. Ozaki, Pro-environmental products: marketing influence on consumer purchase decision, J. Consum. Mark. 25 (2008) 281-293.
46. A.M. Rouhi, Fine chemicals firms enable flavor and fragrance industry, Chem. Eng. News 81 (2003) 54.
47. K.W. Böddeker, G. Bengston, E. Bode, Pervaporation of low volatility aromatics from water, J. Membr. Sci. 53 (1990) 143–158.
48. K.W. Böddeker, G. Bengston, H. Pingel, S. Dozel, Pervaporation of high boilers using heated membranes, Desalination 90 (1993) 249–257.
49. K.W. Böddeker, I.L. Gatfield, J. Jähnig, C. Schorm, Pervaporation at the vapor pressure limit: Vanillin, J. Membr. Sci. 137 (1997)155–158.
50. C. Brazhina, B. Barbosa, G.J. Crespo, Sustainable recovery of pure natural vanillin from fermentation media in a single pervaporation step, Green Chem. 13 (2011) 2197–2203.
51. G. Camera-Roda, V. Augugliaro, V. Loddo, L. Palmisano, Pervaporation membrane reactors, in: A. Basile (Ed.), Handbook of membrane reactors reactor types and industrial applications, Woodhead Publishing Series in Energy, vol. 2, p. 256, 2013.
52. V. Augugliaro, G. Camera-Roda, V. Loddo, G. Palmisano, L. Palmisano, F. Parrino, M.A. Puma, Synthesis of vanillin in water by TiO_2 photocatalysis, Appl. Catal. B 111 (2012) 555-561.
53. K.W. Böddeker, G. Bengtson, H. Pingel, S. Dozel, Pervaporation of high boilers using heated membranes, Desalination 90 (1993) 249–257.
54. G. Camera-Roda, V. Augugliaro, A. Cardillo, V. Loddo, G. Palmisano, L. Palmisano, A pervaporation photocatalytic reactor for the green synthesis of vanillin, Chem. Eng. J. 224 (2013) 136–143.
55. G. Camera-Roda, A. Cardillo, V. Loddo, L. Palmisano, F. Parrino, Improvement of membrane performances to enhance the yield of vanillin in a pervaporation reactor, Membranes, 4 (2014) 96-112.
56. G. Camera-Roda, V. Loddo, L. Palmisano, F. Parrino, F. Santarelli, Process intensification in a photocatalytic membrane reactor: Analysis of the techniques to integrate reaction and separation, Chem. Eng. J. 310 (2017) 352-359.
57. G. Camera-Roda, F. Santarelli, Design of a pervaporation photocatalytic reactor for process intensification, Chem. Eng. Technol. 35 (2012) 1221-1228.
58. O. Levenspiel, Chemical Reaction Engineering, third ed., John Wiley & Sons, New York, 1999.
59. A.I. Stankiewicz, J.A. Moulijn, Process intensification: Trasforming chemical engineering, Chem. Eng. Progr. (2000) 22-34.
60. P.W. Battersby, P.W. Teixeira, J. Beltramini, M.C. Duke, V. Rudolph, J.C. Diniz Da Costa, An analysis of the Peclet number and Damkohler numbers for dehydrogenation reactions using molecular sieve silica (MSS) membrane reactors, Catal. Today 116 (2006) 12–17.
61. W.S. Moon, S.B. Park, Design guide of a membrane for a membrane reactor in terms of permeability and selectivity, J. Membr. Sci. 170 (2000) 43–51.
62. Böddeker, K.W. 1st ed.; Springer-Verlag: Berlin/Heidelberg, pp. 1–146, 2008.
63. A. Fujishima, K. Honda, Electrochemical photolysis of water at a semiconductor electrode, Nature 238 (1972) 37–38.
64. K. Fujihara, T. Ohno, M. Matsumura, Splitting of water by electrochemical combination of two photocatalytic reactions on TiO_2 particles, J. Chem. Soc., Faraday Trans. 94 (1998) 3705-3709.
65. C.C. Lo, C.W. Huang, C.H. Liao, J.C.S Wu, Novel twin reactor for separate evolution of hydrogen and oxygen in photocatalytic water splitting, Int. J. Hydrogen Energ. 35 (2010) 1523–1529.
66. S.C. Yu, C.W. Huang, C.H. Liao, J.C.S. Wu, S.T. Chang, K.H. Chen, A novel membrane reactor for separating hydrogen and oxygen in photocatalytic water splitting, J. Memb. Sci. 382 (2011) 291–299.
67. Y. Sasaki, H. Kato, A. Kudo, $[Co(bpy)_3]^{3+/2+}$ and $[Co(phen)_3]^{3+/2+}$ electron mediators for overall water splitting under sunlight irradiation using Z-scheme photocatalyst system, J. Am. Chem. Soc. 135 (2013) 5441−5449.
68. E. Selli, G.L. Chiarello, E. Quartarone, P. Mustarelli, I. Rossetti, L. Forni, A photocatalytic water splitting device for separate hydrogen and oxygen evolution, Chem. Commun. (2007) 5022–5024.

69. C.H. Liao, C.W. Huang, J.C.S. Wu, Novel dual-layer photoelectrode prepared by RF magnetron sputtering for photocatalytic water splitting, Int. J. Hydrogen Energ. 37 (2012) 11632-11639.

70. B. Seger, P.V. Kamat, Fuel Cell Geared in Reverse: Photocatalytic hydrogen production using a TiO_2/Nafion/Pt membrane assembly with no applied bias, J. Phys. Chem. C 113 (2009) 18946–18952.

71. R. Marschall, C. Klaysom, A. Mukherji, M. Wark, G.Q. Lu, L. Wang, Composite proton-conducting polymer membranes for clean hydrogen production with solar light in a simple photoelectrochemical compartment cell, Int. J. Hydrogen Energ. 37 (2012) 4012-4017.

72. D.E. Tsydenov, V.N. Parmon, A.V. Vorontsov, Toward the design of asymmetric photocatalytic membranes for hydrogen production: preparation of TiO_2-based membranes and their properties, Int. J. Hydrogen Energ. 37 (2012) 11046-11060.

73. D.E. Tsydenov, A.V. Vorontsov, Influence of Nafion loading on hydrogen production in a membrane photocatalytic system, J. Photochem. Photobiol. A: Chem. 297 (2015) 8–13.

74. S. Troppmann, B. König, Functionalized membranes for photocatalytic hydrogen production, Chem. Eur. J. 20 (2014) 14570-14574.

75. F. Della Foglia, G.L. Chiarello, M.V. Dozzi, P. Piseri, L.G. Bettini, S. Vinati, C. Ducati, P. Milani, E. Selli, Hydrogen production by photocatalytic membranes fabricated by supersonic cluster beam deposition on glass fiber filters, Int. J. Hydrogen Energ. 39 (2013) 13098-13104.

76. C. Zamfirescu, I. Dincer, G.F. Naterer, Analysis of a photochemical water splitting reactor with supramolecular catalysts and a proton exchange membrane, Int. J. Hydrogen Energ. 36 (2011) 11273-11281.

77. K. Wu, Z. Chen, H. Lv, H. Zhu, C.L. Hill, T. Lian, Hole removal rate limits photodriven H_2 generation efficiency in CdS-Pt and CdSe/CdS-Pt semiconductor nanorod–metal tip heterostructures, J. Am. Chem. Soc. 136 (2014) 7708-7716.

78. X. Chen, S. Shen, L. Guo, S.S. Mao, Semiconductor-based photocatalytic hydrogen generation, Chem. Rev. 110 (2010) 6503-6570.

79. A. Kubacka, M. Fernández-García, G. Colón, Advanced nanoarchitectures for solar photocatalytic applications, Chem. Rev. 112 (2012) 1555-614.

80. S. Bhattacharyya, L. Polavarapu, J. Feldmann, J.K. Stolarczyk, Challenges and prospects in solar water splitting and CO_2 reduction with inorganic and hybrid nanostructures, ACS Catal. 8 (2018) 3602-3635.

81. W. Lin, H. Han, H. Frei, CO_2 Splitting by H_2O to CO and O_2 under UV Light in TiMCM-41 Silicate Sieve, J. Phys. Chem. B 108 (2004) 18269-18273.

82. G. Qin, Y. Zhang, X. Ke, X. Tong, Z. Sun, M. Liang, S. Xue, Photocatalytic reduction of carbon dioxide to formic acid, formaldehyde, and methanol using dye-sensitized TiO_2 film, Appl. Catal. B Environ. 129 (2013) 599-605.

83. H. Slamet, H.W. Nasution, E. Purnama, S. Kosela, G. Lazuardi, J. Photocatalytic reduction of CO_2 on copper-doped titania catalysts prepared by improved-impregnation method, Catal. Commun. 6 (2005) 313-319.

84. G. Mele, C. Annese, A. De Riccardis, C. Fusco, L. Palmisano, G. Vasapollo, L. D'Accolti, Turning lipophilic phthalocyanines/TiO_2 composites into efficient photocatalysts for the conversion of CO_2 into formic acid under UV–vis light irradiation, Appl. Catal. A: Chem 481 (2014) 169-172.

85. S. Ichikawa, R. Doi, Hydrogen production from water and conversion of carbon dioxide to useful chemicals by room temperature photoelectrocatalysis, Catal. Today 27 (1996) 271-277.

86. J. Premkumar, R. Ramaraj, Photocatalytic reduction of carbon dioxide to formic acid at porphyrin and phthalocyanine adsorbed Nafion membranes, J. Photochem. Photobiol. A: Chem. 110 (1997) 53-58.

87. P. Pathak, M.J. Meziani, Y. Li, L.T. Cureton, Y.P. Sun, Improving photoreduction of CO_2 with homogeneously dispersed nanoscale TiO_2 catalysts, Chem.Commun. (2004) 1234-1235.

88. P. Pathak, M.J. Meziani, L. Castillo, Y.P. Sun, Metal-coated nanoscale TiO_2 catalysts for enhanced CO_2 photoreduction, Green Chem. 7 (2005) 667–670.

89. S. Rani, N. Bao, S.C. Roy, Solar spectrum photocatalytic conversion of CO_2 and water vapor into hydrocarbons using TiO_2 nanoparticle membranes, Appl. Surf. Sci. 289 (2014) 203– 208.

90. X. Cheng, R. Chen, X. Zhu, Q. Liao, X. He, S. Li, L. Li, Optofluidic membrane microreactor for photocatalytic reduction of CO_2, Int. J. Hydrogen Energ. 41 (2016) 2457-2465.

91. M. Sellaro, M. Bellardita, A. Brunetti, E. Fontananova, L. Palmisano, E. Drioli, G. Barbieri, CO_2 conversion in a photocatalytic continuous membrane reactor, RSC Advances 6 (2016) 67418 - 67427.

92. F.R. Pomilla, A. Brunetti, G. Marcì, E.I. Garcia-Lopez, E. Fontananova, L. Palmisano, G. Barbieri, CO_2 to liquid fuels: Photocatalytic conversion in a continuous membrane reactor, ACS Sust. Chem. Eng. 6(7) (2018) 8743–8753.

93. S. Sato, T. Arai, T. Morikawa, K. Uemura, T.M. Suzuki, H. Tanaka, T. Kajino, Selective CO_2 conversion to formate conjugated with H_2O oxidation utilizing semiconductor/complex hybrid photocatalysts, J. Am. Chem. Soc. 133 (2011) 15240–15243.

94. T. Arai, S. Sato, T. Kajino, T. Morikawa, Solar CO_2 reduction using H_2O by a semiconductor/metal-complex hybrid photocatalyst: enhanced efficiency and demonstration of a wireless system using $SrTiO_3$ photoanodes, Energy Environ. Sci. 6 (2013) 1274-1282.

95. W.H. Lee, C.H. Liao, M.F. Tsai, C.W. Huang, J.C.S. Wu A novel twin reactor for CO_2 photoreduction to mimic artificial photosynthesis, Appl. Catal. B 132-133 (2013) 445- 451.

96. Y.H. Cheng, V.H. Nguyen, H.Y. Chan, J.C.S. Wu, W.H. Wang, Photo-enhanced hydrogenation of CO_2 to mimic photosynthesis by CO co-feed in a novel twin reactor, Appl. Energ. 147 (2015) 318–324.

97. S. Li, L. Yang, O. Ola, M. Maroto-Valer, X. Du, Y. Yang, Photocatalytic reduction of CO_2 by CO co-feed combined with photocatalytic water splitting in a novel twin reactor, Energ. Convers. Manage. 116 (2016) 184-193.

98. R. Molinari, C. Lavorato, T.F. Mastropietro, P. Argurio, E. Drioli, T. Poerio, Preparation of Pd-loaded hierarchical FAU membranes and testing in acetophenone hydrogenation, Molecules 21(2016) 394.

99. R. Molinari, C. Lavorato, P. Argurio, Photocatalytic reduction of acetophenone in membrane reactors under UV and visible light using TiO_2 and Pd/TiO_2 catalysts, Chem. Eng. J. 274 (2015) 307–316.

100. K. Imamura, S. Iwasaki, T. Maeda, K. Hashimoto, B. Ohtani, H. Kominami, Photocatalytic reduction of nitrobenzenes to aminobenzenes in aqueous suspensions of titanium(IV) oxide in the presence of hole scavengers under deaerated and aerated conditions, Phys. Chem. Chem. Phys. 13 (2011) 5114–5119.

101. N. Wehbe, M. Jaafar, C. Guillard, J.-M. Herrmann, S. Miachon, E. Puzenat, N.Guilhaume, Comparative study of photocatalytic and non-photocatalytic reduction of nitrates in water, Appl. Catal. A Gen. 368 (2009) 1–8.

102. A. Pandikumar, S. Manonmani, R. Ramaraj, TiO_2–Au nanocomposite materials embedded in polymer matrices and their application in the photocatalytic reduction of nitrite to ammonia, Catal. Sci. Technol. 2 (2012) 345–353.